

Interpreting Neural Policies with Disentangled Tree Representations

Tsun-Hsuan Wang*, Wei Xiao, Tim Seyde, Ramin Hasani, Daniela Rus

Massachusetts Institute of Technology (MIT)

Compact neural networks used in policy learning and closed-loop end-to-end control learn representations from data that encapsulate agent dynamics and potentially the agent-environment’s factors of variation. A formal and quantitative understanding and interpretation of these explanatory factors in neural representations is difficult to achieve due to the complex and intertwined correspondence of neural activities with emergent behaviors. In this paper, we design a new algorithm that programmatically extracts tree representations from compact neural policies, in the form of a set of logic programs grounded by world state. To assess how well networks uncover dynamics of the task and their factors of variation, we introduce interpretability metrics that measure disentanglement of learned neural dynamics from a concentration of decisions, mutual information and modularity perspectives. Moreover, our method allows us to quantify how accurate the extracted decision paths (explanations) are and computes cross-neuron logic conflict. We demonstrate the effectiveness of our approach with several types of compact network architectures on a series of end-to-end learning to control tasks.

1. Introduction

In representation learning, we assume that neural networks capture a set of processes that exist in the data distribution. However, we do not have access to these *factors of variation* explicitly as they are encoded by neural activities. Ideally, we wish to learn representations that contain informative and useful features (Bengio et al., 2013), while being semantically meaningful and interpretable.

In this regard, it has been shown that better representations can be learned if they are disentangled (Locatello et al., 2019; Peters et al., 2017; Schmidhuber, 1992). Although, in unsupervised learning and semi-supervised learning we could measure the disentanglement with various metrics (Locatello et al., 2019; Schölkopf et al., 2021), in general it is difficult to identify and understand these disentangled representations as they are encoded in complex neural dynamics corresponding to network’s behavior.[†]

In the present study, we aim to explore how to uncover dynamics and factors of variation quantitatively in compact neural networks used in policy learning and closed-loop end-to-end control. In this space, an entangled correspondence to multiple neurons responsible for an emergent behavior can obstruct the interpretation of neuron response even with a small number of neurons (Hasani et al., 2021b; Lechner et al., 2019, 2020a; Vorbach et al., 2021). To this end, the disentanglement of learned representations in compact neural networks is essential for deriving explanations and interpretations for neural policies.

We posit that each neuron should learn an abstraction (factor of variation) related to a specific strategy required for solving a sub-component of a task. For example, in locomotion, one neuron may capture periodic gait, where numerical value of the neuron response may be aligned with different phases of gait cycle; another neuron may account for recovery from slipping. On the other hand, directly observing numerical values of the neuron

*Correspondence E-mail: tsunw@mit.edu

[†]This is true as long as we do not have the causal structure of the task (Schölkopf et al., 2021).

response along with sensory information provided as input to the policy can be extremely inefficient and tedious for identifying behaviors and interpreting decision making.

In this work, our objective is to formulate a logic program that represents the decision-making of a parametric policy to improve interpretability of learned behaviors.

To this end, we make the following key **contributions**:

- A novel algorithm that programmatically extracts tree representations from compact neural policies, in the form of a set of logic programs grounded by world state.
- Introducing a novel series of quantitative metrics of interpretability to assess how well networks uncover dynamics of the task and their factors of variation. These methods include measure disentanglement of learned neural dynamics from a concentration of decisions, mutual information and modularity perspectives.
- Quantifying the accuracy of the extracted decision paths and computing cross-neuron logic conflicts.
- Extensive experimental evaluation of our method in a series of end-to-end learning to control tasks.

2. Related Work

Interpreting neural networks. A survey for interpretable neural networks is given in (Hasani, 2020; Zhang et al., 2021). An interpretable neural network could be constructed from a physically comprehensible perspective (Hasani et al., 2019; Toms et al., 2020). Self-explaining neural networks have been proposed in (Alvarez Melis and Jaakkola, 2018) to achieve robust interpretability of the model, in which explicitness, faithfulness, and stability (Lechner et al., 2020b) are the main considerations. Knowledge representation is used in convolutional layers to obtain interpretable CNNs (Babaiee et al., 2021; Lechner et al., 2022; Sietzen et al., 2021; Zhang et al., 2018). Another active line of research is to study disentangled explanatory factors in learned representation (Locatello et al., 2019). A better representation should contain information in a compact and interpretable structure (Bengio et al., 2013; Chen et al., 2018a; Hasani et al., 2017). Unlike prior works that study disentanglement based on *factors of variations* in the data such as object types, there is no notion of ground-truth factors in policy learning (Brunnbauer et al., 2022; Hasani et al., 2020) and thus we propose to use tree-based representation to construct a pseudo-ground-truth factor set that captures emergent behaviors of neural policies for interpretability analysis.

Decision trees in interpretable neural networks. Decision trees have been used to interpret CNN from observation to filters (Chyung et al., 2019; Zhang et al., 2019). Decision trees can also help compress a model by determining the number of hidden layers of a deep neural network (Schaaf et al., 2019; Ueno and Zhao, 2018; Wu et al., 2021). Accuracy and interpretability of a model may often contradict each other and induce a traded-off. One can improve both by adding a differentiable decision tree to the last layer of a neural network (Wan et al., 2021). All the related prior works aim to interpret a neural network at the high level, while in this paper, we interpret a neural network at the neuron level, which is especially important and useful for safety-critical applications (DelPreto et al., 2020; Grunbacher et al., 2021; Hasani et al., 2016; Lechner et al., 2021; Xiao et al., 2021, 2022a). The neuron level interpretation can also help us understand why a model fails to work.

3. Compact Networks for Neural Policies

To obtain compact neural representations, there are three common approaches: 1) simply choose an RNN with small number of units densely wired to each other (e.g., a long short-term memory, LSTM (Hochreiter and

Schmidhuber, 1997), or a continuous-time network such as an ordinary differential equation (ODE)-based network (Chen et al., 2018b; Lechner and Hasani, 2020; Rubanova et al., 2019)). 2) sparsify a large network into a smaller system (e.g., lottery ticket winners (Frankle and Carbin, 2018), or sparse flows (Babaiee et al., 2022; Liebenwein et al., 2021b)), and 3) use neural circuit policies that are given by sparse architectures with added complexity to their neural and synaptic representations but have a light-weighted network architecture (Hasani et al., 2021a,b; Lechner et al., 2020a).

In the first approach the number of model parameters inversely affect interpretability, i.e., interpreting wider and/or deeper densely wired RNNs exponentially makes the interpretation of the system harder. Sparsity has been shown to help obtain a network with 95% less parameters compared to the initial model. However, recent studies show that such levels of sparsity affect the robustness of the model, thus make it more susceptible to perturbations (Liebenwein et al., 2021a). Neural circuit policies (NCPs) (Lechner et al., 2020a) on the other hand have shown great promise in achieving attractive degrees of generalizability while maintaining robustness to environmental perturbations. This representation learning capability is rooted in their ability to capture the true cause and effect of a given task (Vorbach et al., 2021). NCPs are sparse network architectures with their nodes and edges determined by a liquid time-constant (LTC) concept (Hasani et al., 2021b). The state of a liquid network is described by the following set of ODEs (Hasani et al., 2021b): $\frac{d\mathbf{x}(t)}{dt} = -\left[\frac{1}{\tau} + f(\mathbf{x}(t), \mathbf{I}(t), t, \theta)\right] \odot \mathbf{x}(t) + f(\mathbf{x}(t), \mathbf{I}(t), t, \theta) \odot A$. Here, $\mathbf{x}^{(D \times 1)}(t)$ is the hidden state with size D , $\mathbf{I}^{(m \times 1)}(t)$ is an input signal, $\tau^{(D \times 1)}$ is the fixed internal time-constant vector, $A^{(D \times 1)}$ is a bias parameter, and \odot is the Hadamard product. In tasks involving spatiotemporal dynamics these networks showed significant benefit over their counterparts (Hasani et al., 2022), both in their ODE form and in their closed-form representation termed Closed-form continuous-time (CfC) models (Hasani et al., 2021a; Lechner et al., 2020a; Vorbach et al., 2021). In the following we dissect the inner dynamics of these models based on decision trees.

4. Interpretability of Compact Neural Policies

4.1. Interpretation based on Neuron Response

Compact neural representations promise to enable interpretability of decision-making by focusing post-hoc analysis on a limited number of neural responses.

However, having merely a lower-dimensional space for visualization is not sufficient to identify consistent behaviors or strategies acquired by a learning agent. Emergent behaviors may distribute responses across numerous neurons with a high degree of entanglement. Even for models with a small number of neurons, it can be challenging to identify and interpret the behavior correlated with observed response patterns. In this paper we hypothesize that abstraction with respect to a type of learned strategy within a single neuron is necessary for better interpretability of neural policies. We further desire semantic grounding of the neuron response, that is, associating neuron response to human-readable representation. The representation space should be abstract enough to be human-understandable and expressive enough to capture arbitrary types of emergent behaviors or strategies. We adopt the framework of logic programs due to their simple yet effective representations of decision making processes.

4.1.1. Preliminaries

Building on the considerations in the previous section, we describe a decision process as a tuple $\{\mathcal{O}, \mathcal{S}, \mathcal{A}, P_a, h\}$, where at a time instance t , $o_t \in \mathcal{O}$ is the observation, $s_t \in \mathcal{S}$ is the state, $a_t \in \mathcal{A}$ is the action, $P_a : \mathcal{S} \times \mathcal{A} \times \mathcal{S} \rightarrow$

Algorithm 1: Interpreter for Neural Policies

Data: Trajectories rollout from a compact neural policy $\mathcal{D}_{dt} = \{(o_0, s_0, a_0, z_0, \dots)_j\}_{j=1}^N$
Result: Interpreters of neuron response $\{f_{\mathcal{S}}^i\}_{i \in \mathcal{I}}$
for $i \in \mathcal{I}$ **do**
 Train a decision tree T_{θ^i} from state $\{s_t\}$ to neuron response $\{z_t^i\}$;
 Collect dataset \mathcal{D}_{dp} with neuron response $\{z_t^i\}$ and decision paths $\{\mathcal{P}_{s_t}^i\}$;
 Train neuron response classifier $q_{\theta^i} : \mathbb{R} \rightarrow \{\mathcal{P}\}$ with \mathcal{D}_{dp} ;
 Obtain decision path parser $r^i : \{\mathcal{P}\} \rightarrow \mathcal{L}$ by tracing out $\{\mathcal{P}_k^i\}_{k=1}^{K^i}$ in T_{θ^i} ;
 Construct interpreter $f_{\mathcal{S}}^i = r^i \circ q_{\theta^i}$;
end

$[0, 1]$ is the transition probability from current state s_t to next state s_{t+1} under action a_t , and $h : \mathcal{S} \rightarrow \mathcal{O}$ is the observation model. We define a neural policy as $\pi : \mathcal{O} \rightarrow \mathcal{A}$ and the response of neuron $i \in \mathcal{I}$ as $\{z_t^i \in \mathbb{R}\}_{i \in \mathcal{I}}$, where \mathcal{I} refers to a set of neurons to be interpreted. For each neuron i , our goal is to construct an interpreter grounded in the set of environment states \mathcal{S} that, from neuron response z_t^i , infers a logic program $f_{\mathcal{S}}^i : \mathbb{R} \rightarrow \mathcal{L}$, where \mathcal{L} is a set of logic programs. Note that the interpreter is only grounded in the state space by defining variables used in logic formulae, however, it does not take state as an input as underlying states may be inaccessible during inference.

4.2. Decision Trees as the Basis for Logic Programs

Our goal is to formulate a logic program that represents the decision-making of a parametric policy to improve interpretability of learned behaviors. We propose to first extract the underlying decision tree from the policy which can then be leveraged to construct an interpreter $l_t^i = f_{\mathcal{S}}^i(z_t^i)$, where $l_t^i \in \mathcal{L}$ is a logic program.

Decision trees are non-parametric supervised learning algorithms for classification and regression. Throughout training, they develop a set of decision rules based on thresholding one or a subset of input dimensions. The relation across rules is described by a tree structure with the root node as the starting point of the decision making process and the leaf nodes as the predictions for classification or regression. The property of decision trees to convert either categorical or continuous-valued data to a set of propositions is a natural fit to state-grounded logic programs. Given an off-the-shelf trained neural policy π , we collect a set of rollout trajectories $\mathcal{D}_{dt} = \{\tau_j\}_{j=1}^N$, where $\tau_j = (o_0, s_0, a_0, z_0, o_1, s_1, a_1, z_1 \dots)$. We first train a decision tree T_{θ^i} to predict the t 'th neuron response based on state,

$$\theta^{i*} = \arg \min_{\theta^i} \sum_{(s_t, z_t^i) \in \mathcal{D}_{dt}} L_{dt}(\hat{z}_t^i, z_t^i), \text{ where } \hat{z}_t^i = T_{\theta^i}(s_t) \quad (1)$$

where L_{dt} represents the underlying classification or regression criteria. The decision tree T_{θ^i} describes relations between the neuron responses and the relevant states in terms of logical expressions.

During inference, starting from the root node, relevant state dimensions will be checked by the decision rule in the current node and directed to the relevant lower layer, finally arriving at one of the leaf nodes and providing information to regress the neuron response. Each inference essentially traces out a route from the root node to a leaf node. This route is called a decision path. A decision path consists of a sequence of decision rules defined by nodes visited by the path, which combine to form a logic program,

$$\bigwedge_{n \in \mathcal{P}_{s_t}^i, j=g(n)} (s_t^j \leq c_n) \longleftrightarrow \text{Info for } \hat{z}_t^i \quad (2)$$

where \wedge is the logical AND, $\mathcal{P}_{s_t}^i$ is the decision path of tree T_{θ^i} that takes s_t as inputs, g gives the state dimension used in the decision rule of node n (we assume each node uses only one feature for notation simplicity), and c_n is the threshold at node n . This enables us to recover a correspondence between the neuron response and the state-grounded program; however, this approach is not sufficient for deployment since the decision tree T_{θ^i} requires as input the ground-truth state rather than the data that is observable by the policy (like o_t, z_t). To address this, we find an inverse of T_{θ^i} . Based on the inference process, there is a one-to-one correspondence between \hat{z}_t^i and $\mathcal{P}_{s_t}^i$, thus z_t^i and $\mathcal{P}_{s_t}^i$. We can then collect another dataset \mathcal{D}_{dp} based on the inference of T_{θ^i} and train a classifier q_{ϕ^i} to predict decision paths from neuron responses,

$$\phi^{i*} = \arg \min_{\phi^i} \sum_{(z_t^i, \mathcal{P}_{s_t}^i) \in \mathcal{D}_{dp}} L_{dp}(q_{\phi^i}(z_t^i), \mathcal{P}_{s_t}^i) \quad (3)$$

where L_{dp} is a classification criterion. While $\mathcal{P}_{s_t}^i$ is state-dependent, there exists a finite set of decision paths $\{\mathcal{P}_k^i\}_{k=1}^{K^i}$ given the generating decision tree. We define the mapping from the decision tree to the logic program as $r : \{\mathcal{P}\} \rightarrow \mathcal{L}$, which can be obtained by tracing out the path as described above. The interpreter is readily constructed using the mapping and the classifier $f_S^i = r^i \circ q_{\phi^i}$. The overall procedure is summarized in Algorithm 1.

4.3. Quantitative Measures of Interpretability

Programmatically extracting decision trees for constructing a mapping from the neuron response to a logic program offers a representation that facilitates the interpretability of compact neural policies. Furthermore, building on the computational aspect of our approach, we can quantify the interpretability of a model with respect to several metrics.

A. Disentanglement. We have described how well an individual neuron response can be associated with a specific behavior or strategy. This association is important for the interpretability of a compact neural policy, and it can be viewed as the disentanglement of the learned representation along the feature dimensions.

1. Neuron-Response Variance. Given the finite set of decision paths $\{\mathcal{P}_k^i\}_{k=1}^{K^i}$ associated with a tree T_{θ^i} , we first compute the average normalized variance of the neuron response corresponding to each decision path,

$$\frac{1}{|\mathcal{I}|} \sum_{i \in \mathcal{I}} \frac{1}{K^i} \sum_{k=1}^{K^i} \text{Var}_{\substack{(s_t, z_t^i) \in \mathcal{D}_{dt} \\ t \in \{u | \mathcal{P}_{s_u}^i = \mathcal{P}_k^i\}}} \left[\frac{z_t^i}{Z^i} \right] \quad (4)$$

where Z^i is a normalization factor that depends on the range of response of the i 'th neuron. In practice, we discretize all neuron responses to N bins, compute the index of bins to which a value belongs, divide the index by N and compute their variance. This metric captures the concentration of the neuron response that corresponds to the same strategy represented by the logic program defined by T_{θ^i} .

2. Mutual Information Gap. Additionally, inspired by (Locatello et al., 2019), we integrate the notion of mutual information in our framework to extend disentanglement measures for unsupervised learning to policy learning. Specifically, while previous literature assumes known ground-truth factors for disentanglement such as object types, viewing angles, etc., there is no straightforward equivalence in neural policies since the emergent behaviors or strategies are unknown priori. To this end, we propose to leverage the decision path sets to construct pseudo ground-truth factors \mathcal{M}_{dp} ,

$$\mathcal{M}_{dp} = \bigcup_{i \in \mathcal{I}} \{\mathcal{P}_k^i\}_{k=1}^{K^i} = \{\mathcal{P}_k\}_{k=1}^K \quad (5)$$

Note that there may be correlation across decision paths, i.e., $P(\mathcal{P}_i, \mathcal{P}_j) \neq P(\mathcal{P}_i)P(\mathcal{P}_j)$ for $i \neq j$. For example, one decision path corresponding to a logic program of the robot moving forward at high speed has correlation to another decision path for moving forward at low speed. Such a situation may occur because a neuron of a policy can learn arbitrary behaviors. However, this leads to a non-orthogonal ground-truth factor set and can be undesired since high correlations of a neuron to multiple ground-truth factors (e.g., $I[z^i; \mathcal{P}_i]$ and $I[z^i; \mathcal{P}_j]$ are large) can result from not only entanglement of the neuron but also the correlation between factors (e.g., $I[\mathcal{P}_i; \mathcal{P}_j]$ is large). Hence, this urges the need to calibrate mutual information for computing disentanglement measure. We start by adapting the Mutual Information Gap (MIG) (Chen et al., 2018a) to our framework:

$$\frac{1}{K} \sum_{k=1}^K \frac{1}{H[\mathcal{P}_k]} \left(I[z^{i^*}; \mathcal{P}_k] - \max_{j \neq i^*} I[z^j; \mathcal{P}_k] - I[z^j; \mathcal{P}_k; \mathcal{P}_{k^j}] \right) \quad (6)$$

where H is entropy, I is interaction information that can take arbitrary number of variables (with 2 being mutual information), $i^* = \arg \max_i I[z^i; \mathcal{P}_k]$, and $k^j = \arg \max_l I[z^j; \mathcal{P}_l]$. Intuitively, this measures the normalized difference between the highest and the second highest mutual information of each decision path with individual neuron activation. The last term $I[z^j; \mathcal{P}_k; \mathcal{P}_{k^j}]$ captures the inherent correlation between z^j and \mathcal{P}_k resulted from potentially nonzero $I[\mathcal{P}_k; \mathcal{P}_{k^j}]$ with \mathcal{P}_{k^j} being a proxy random variable of z^j in the ground-truth factor set.

3. Modularity. We compute modularity scores adapted from (Ridgeway and Mozer, 2018) with the same calibration term,

$$\frac{1}{\mathcal{I}} \sum_{i \in \mathcal{I}} 1 - \frac{\sum_{k \neq k^*} (I[z^i; \mathcal{P}_k] - I[z^i; \mathcal{P}_k; \mathcal{P}_{k^*}])^2}{(K-1)I[z^i; \mathcal{P}_{k^*}]^2}, \quad (7)$$

where $k^* = \arg \max_l I[z^i; \mathcal{P}_l]$. In a modular representation, each neuron depends on at most a single factor of variation. Suppose for each neuron i has the best "match" with a decision path (ground-truth factor) k^* , non-modularity of that neuron is computed as the normalized variance of mutual information between its neuron response and all non-matched decision paths $\{\mathcal{P}_k\}_{k \neq k^*}$. We then discretize neuron responses into N bins to construct categorical distributions for computing discrete mutual information.

Lemma 1. *The calibration term $I[z^j; \mathcal{P}_k] - I[z^j; \mathcal{P}_k; \mathcal{P}_{k^j}]$ in both MIG (6) and Modularity (7) metrics, for $j \neq i^*$, without loss of generality has the following lower bound:*

$$I[z^j; \mathcal{P}_k] - I[z^j; \mathcal{P}_k; \mathcal{P}_{k^j}] \geq \max(0, I[z^j; \mathcal{P}_k] - I[\mathcal{P}_k; \mathcal{P}_{k^j}]) \quad (8)$$

The proof is provided in Appendix. Lemma 1 is necessary, because to compute the calibration term, we need access to the conditional distribution of the random variable $(\mathcal{P}_{k^j} | z^j)$, which is normally inaccessible. Hence, we derive a lower bound for the calibrated mutual information.

B. Decision Path Accuracy. During deployment, we use an inverse proxy q_{ϕ^i} for the decision tree T_{θ^i} and hence we compute the approximation error by measuring the accuracy of a state-grounded decision path inferred from the neuron response with q_{ϕ^i} compared to true states,

$$\frac{1}{|\mathcal{I}|} \sum_{i \in \mathcal{I}} \frac{1}{|\mathcal{D}_{\text{dt}}|} \sum_{(s_t, z_t^i) \in \mathcal{D}_{\text{dt}}} \frac{1}{|q_{\phi^i}(z_t^i)|} \sum_{\substack{n \in q_{\phi^i}(z_t^i) \\ j=g(n)}} \mathbb{1}[s_t^j \leq c_n] \quad (9)$$

where $\mathbb{1}$ is an indicator function. Note that the discrepancy is computed at the decision rule level. Thus it captures not only the error of the classifier model q_{ϕ^i} but also how accurately f_S^i parses z_t^i .

C. Cross-neuron Logic Conflict. When interpreting a neural policy as a whole instead of inspecting individual neuron response, it is straightforward to find the intersection across logic programs extracted from different

neurons $l_t = \text{reduce}(\bigwedge_{i \in \mathcal{I}} l_t^i)$, where `reduce` is a intuitively, the neuron-wise logic program that should summarize the operational domain of the strategy currently executed by the neuron, where intersection describes the domain of a joint strategy across neurons. However, the reduction of intersection can be invalid if there is conflict on the logical formulae across neurons, e.g., $a \leq 3$ from the first neuron and $a \geq 4$ from the second neuron. The conflict may imply, under the same configuration of f_S , that (1) the policy fails to learn compatible strategies across neurons or (2) there is error induced by the interpreter due to insufficient or ambiguous connection between the logic program and the neuron response, which implicitly indicates interpretability of a policy.

5. Experiments

In this section, we conduct a series of end-to-end learning to control experiments on which we evaluate our interpretability methods and metrics, comprehensively.

Network Architecture Priors. We construct compact neural networks for each end-to-end learning to control task. For all tasks, our networks are constructed by the following priors: (i) Each baseline network is supplied with a perception backbone (e.g., a convolutional neural network) (ii) We construct policies based on different compact architectures that take in feature vectors from the perception backbone and output control with comparable cell counts (instead of actual network size in memory as we assess interpretability metrics down to cell-level) (iii) for multi-layer architectures, force a layer to have few neuron count for interpretation.

Baselines. The perception backbone is followed by a neural controller designed by compact feed-forward and recurrent network architectures including fully-connected network (**FCs**), gated recurrent units (**GRU**) (Cho et al., 2014), and long-short term memory (**LSTM**) (Hochreiter and Schmidhuber, 1997). Additionally, we include advanced continuous-time baselines designed by ordinary differential equations such as **ODE-RNN** (Rubanova et al., 2019), closed-form continuous-time neural models (**CfCs**) (Hasani et al., 2021a), and neural circuit policies (**NCPs**) (Lechner et al., 2020a). NCPs are designed by a four-layer structure consisting of sensory neurons (input layer), interneurons, command neurons (with recurrent connections), and motor neuron (output layer). To make a fair comparison, we augment a feed-forward layer for other models, which is of equivalent size to the inter-neuron layer in NCPs. We interpret the dynamics of the neurons in the last layer before the output in FCs, the recurrent state of GRUs, LSTMs, ODE-RNNs, and CfCs, and the command-neuron layer of NCPs. We then measure interpretability quantitatively based on our metrics and extract logic programs from cells.

5.1. Case Study 1. Classical Control

Environment and policy learning. We use the OpenAI Gym Classical Control Pendulum task (Brockman et al., 2016). The environment has simple yet nonlinear dynamics, and allows for a straightforward visualization of the entire state space. The environment states include θ (joint angle) and $\dot{\theta} = d\theta/dt$ (joint angular velocity). θ is in the range of $\pm\pi$ with $\theta = 0$ as upright position. $\dot{\theta}$ means velocity along clockwise direction. The control is u (joint torque). The goal is to stabilize at the upright position ($\theta = \dot{\theta} = 0$) with limited control energy consumption ($u \downarrow$). We use Proximal Policy Optimization (PPO) (Schulman et al., 2017) to train the policy with early stop by reaching episode reward -500 or maximal number of training iterations. For each model, we run 5 trials with different random seeds and report average results.

Quantitative analysis. In Table 1, we present results based on the quantitative metrics of interpretability. First, all models achieve comparable performance when learning toward target -500 episode reward except for a subset of models where individual random seeds learn slower and fails to reach the target performance within the

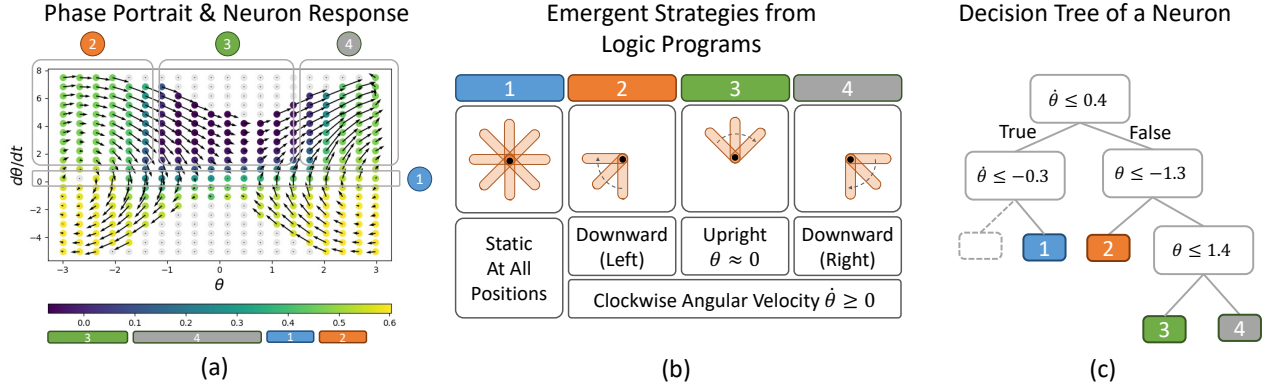


Fig. 1: Interpretation of compact neural policies in classical control (Pendulum). (a) Phase portrait with empirically measured closed-loop dynamics and neuron response. Each arrow and colored dot are the results averaged around the binned state space. (b) Emergent strategies from logic programs. (c) Decision tree extracted for neuron response of command neuron 3 in NCP.

Table 1: Quantitative results of classical control.

Network Arch.	Disentanglement			Decision Path Accuracy \uparrow	Logic Conflict \downarrow	Performance \uparrow
	Variance \downarrow	MI-Gap \uparrow	Modularity \uparrow			
FCs	0.0242	0.3008	0.9412	0.3015	0.2104	-488.55
GRU	0.0329	0.2764	0.9096	0.2504	0.2832	-559.82
LSTM	0.0216	0.2303	0.9355	0.2392	0.5072	-467.95
ODE-RNN	0.0287	0.3062	0.9376	0.2980	0.2506	-533.93
CfC	0.0272	0.2892	0.9067	0.2509	0.1556	-489.28
NCP	0.0240	0.3653	0.9551	0.4726	0.2026	-556.64

maximal training iterations. We observe that NCPs achieve higher scores in disentanglement and decision path accuracy, suggesting that it can yield reliable logic programs with the proposed interpreter. Another interesting finding is that CfCs have the lowest logic conflict. By empirically checking the decision trees, they construct non-trivial but highly-overlapping decision paths, thus leading to considerably fewer conflicts in logic programs across neurons compared to other architectures.

Interpretation of neural policies. While all models learn reasonable strategies, as exemplified by focusing on the sign of θ and $\dot{\theta}$, we now dive deeper into understanding individual neural dynamics. To do this, we pick NCPs as they provide a lower variance from the disentanglement perspective in their logic programs. We found different neurons roughly subdivide the state space into quadrants and focus on their respective subsets. In Figure 1, we show the interpretability analysis of command neuron 3 as an example. This neuron developed fine-grained strategies for different situations like swinging clockwise in the right or left downward positions, and to stabilize positive angular velocity around the upright position, as shown Figure 1 (b)(c). We further provide phase portrait in Figure 1 (a). The arrows indicate empirically measured closed-loop dynamics (with control from the policy) and the color coding indicates average neuron response at a specific state from evaluation. The color of neuron response (which can correspond to logic programs) and the arrows (which implicitly capture actions) highlight different fine-grained strategies in the phase portrait. Note that this finding is not limited to NCPs, and could be observed in other network architectures with similar functions as well.

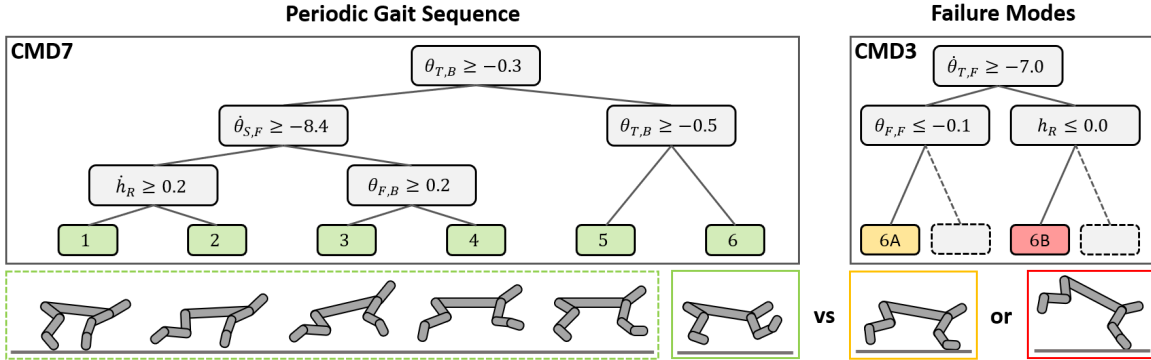


Fig. 2: Qualitative neural activation along a gait sequence on the OpenAI Gym HalfCheetah locomotion task (Brockman et al., 2016). We focus on command neuron 7 and 3 for illustrative purposes. Command neuron 7 exhibits a periodic activation pattern that reacts to different phases of the gait cycle (left). Command neuron 3 displays peak activity in situations with the potential to destabilize gait, such as early touchdown (left) and forward flipping (right). Our approach can therefore help to facilitate failure detection by monitoring responses of individual key neurons.

Table 2: Quantitative results of locomotion.

Network Arch.	Disentanglement			Decision Path Accuracy \uparrow	Logic Conflict \downarrow	Performance \uparrow
	Variance \downarrow	MI-Gap \uparrow	Modularity \uparrow			
FCs	0.0187	0.1823	0.9622	0.5285	0.1035	5186.50
GRU	0.0259	0.1830	0.9713	0.4924	0.1500	3857.21
LSTM	0.0108	0.1453	0.9600	0.5283	0.2155	4122.74
ODE-RNN	0.0210	0.1880	0.9701	0.4959	0.1474	3472.69
CfC	0.0234	0.1596	0.9628	0.4841	0.1581	5195.46
NCP	0.0107	0.2164	0.9791	0.5859	0.1105	5822.73

5.2. Case Study 2: Locomotion

Environment and policy learning. We consider a planar locomotion task based on OpenAI Gym’s HalfCheetah environment (Brockman et al., 2016). The agent is rewarded for forward locomotion based on a simple base velocity reward. We optimize our policies with PPO until a maximum number of episodes has been reached. For each model, we run five trials with different random seeds and report average results. Here, our objective is to extend our interpretability framework to a higher-dimensional control task. Specifically, we investigate whether our approach is capable of extracting consistent single-neuron activation patterns that align with individual phases of a periodic gait cycle.

Quantitative Analysis. We compare quantitative metrics of interpretability across various algorithms in Table 2. We first note that the NCP model compares favorably to the other agents in terms of performance. Furthermore, similar to the classical control experiment, the NCP model achieves higher scores across all interpretability metrics. In conjunction with the proposed interpreter, we find the resulting logic program to offer a high degree of reliability. We further observe that the LSTM desirably achieves low disentanglement variance which is comparable to NCPs. LSTMs and most networks compared to NCPs on the other hand show lower Mutual Information Gap. This suggests that in these networks neuron responses are concentrated for different decision paths but not quite identifiable from a probabilistic perspective, as certain neuron activation cannot be uniquely mapped to a decision path. These results further highlight the importance of using several metrics to capture different aspects of studying interpretability of neural policies.

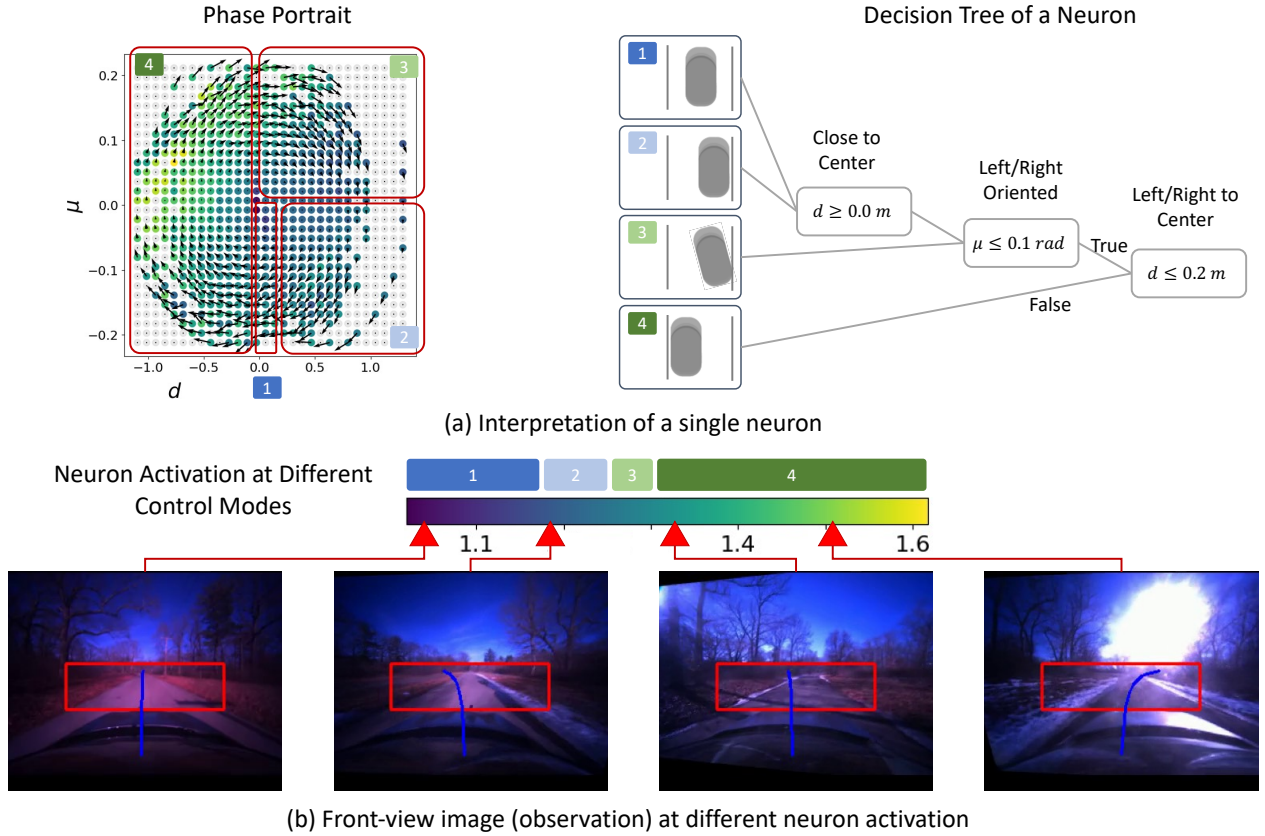


Fig. 3: Interpretation of compact neural policies for end-to-end visual servoing (Image-based Driving). (a) Phase portrait of local heading error μ and lateral deviation d with empirically measured mean neuron response and closed-loop dynamics. (b) Images retrieved based on neuron response.

Qualitative Analysis. As the state-space is significantly larger than the Pendulum task, we complement our quantitative interpretability results with qualitative results that focus on two exemplary neurons, namely command-neurons 3 and 7. Figure 2 provides the extracted decision trees for command neurons 7 (left) and 3 (right). We find that the former displays periodic activation patterns that align very well with individual phases of regular gait. In particular, it leverages position readings of the back thigh joint in conjunction with fore shin velocity to coarsely differentiate between stance and flight phase. More fine-grained coordination of lift-off and touchdown is handled by the leftmost and rightmost branches, respectively. In addition to periodic neuron activations following regular gait, we also observe more specialized decision trees that respond to potential safety-critical situations (Gruenbacher et al., 2022; Xiao et al., 2022b). For example, the decision tree of command neuron 3 includes two branching options that align with variations of tripping due to premature touchdown during flight phase corresponding to a forward trip (6A) and a forward flip (6B). Monitoring the respective activation ranges of command neuron 3 can therefore serve as a proxy for failure detection.

5.3. Case Study 3: End-to-end Visual Servoing

Environment and policy learning. We consider vision-based end-to-end autonomous driving where the neural policy learns to steering commands for lane-following. The model takes front-view RGB images of the vehicle

Table 3: Quantitative results of end-to-end visual servoing.

Network Arch.	Disentanglement			Decision Path Accuracy \uparrow	Logic Conflict \downarrow	Performance \uparrow
	Variance \downarrow	MI-Gap \uparrow	Modularity \uparrow			
FCs	0.0124	0.1354	0.9704	0.5379	0.1354	1.0000
GRU	0.0158	0.1614	0.9801	0.6160	0.1884	0.9210
LSTM	0.0172	0.1950	0.9851	0.5174	0.4504	1.0000
ODE-RNN	0.0151	0.1588	0.9766	0.5483	0.3786	0.4239
CfC	0.0191	0.1391	0.9677	0.5549	0.2274	0.9922
NCP	0.0068	0.3902	0.9770	0.5960	0.1067	1.0000

Table 4: Removing a single neuron based on decision tree interpretation.

Remove Neuron	0	1	2	3	4	5	6	7
Performance \uparrow	0.24	0.07	0.09	1.00	0.969	0.29	0.03	1.00

as input, and outputs controls for steering wheel and speed. We use the high-fidelity data-driven simulator *VISTA* (Amini et al., 2022) as our environment. The simulation is built upon a pre-collect real-world dataset, consisting of approximately 2-hour real-world driving data collected during different times of a day, weather conditions, and seasons of a year, and synthesizes sensory measurement with respect to actions taken by a policy (which can be different from the human log) in a closed-loop setting. We adopt a training strategy called *guided policy learning* that leverages *VISTA* to augment a real-world dataset with diverse synthetic data for robust policy learning. The high-level idea is to exploit the capability of sensor synthesis locally around real-world data and trace out diverse trajectories using a privileged controller with access to ground-truth states. Training labels are generated using nonlinear model predictive control (NMPC), which is computationally expensive yet tractable offline. The training dataset contains roughly 200k image-and-control pairs and mean squared error is used as training objective.

Quantitative analysis. In Table 3 we show a numerical comparison of how various types of compact neural policies can yield different levels of interpretability. We initialize the vehicle at random position throughout the entire track and evaluate the policy for 100 frames (roughly 10s) for 100 episodes. The performance is estimated as the ratio of the length of path traversed without crash and the total path length. All models achieve good performance (≥ 0.9) except for ODE-RNN, which fails to learn a good policy within maximal training iterations. Consistent with previous case-studies, we observe considerably lower disentanglement variance from NCPs and higher MIG scores. A lower variance corresponds to better concentration of neural responses to the same strategy represented by the logic program defined by each tree. A higher MIG score indicates that individual neurons learn more disentangled representations. Thus, their activities are more identifiable.

Removal of neuron based on interpretation. There exist some neurons with logic programs that are sensible but may have little effect on task performance. For example, in NCPs (not confined to this specific architecture but just focus on it for discussion), we find a neuron that aligns its response purely with vehicle speed. Given the task objective is lane following without crashing, such neuron pays attention to useful (for temporal reasoning across frames) but relatively unnecessary (to the task) information. Furthermore, there are neurons that don’t exhibit sufficient correlation with any of the environment state and fail to induce decision branching. In light of these observation, we try to remove neurons that we suspect to have little influence on the performance by inspecting their logic program. We show the results in Table 4. Removing neuron 3, 4, and 7 have marginal impact on task performance. Among them, neuron 3 and 4 mostly depends on vehicle speed v while slightly depends on lateral deviation d from the lane center and neuron 7 fails to split a tree.

6. Conclusion

In this work, we describe a novel approach that programmatically extracts tree representations from compact neural policies, in the form of a set of logic programs grounded by world state. To computationally unveil the decision making aspect of neural policies, we propose a set of quantitative metrics that measures disentanglement of learned neural responses from a concentration of decisions, mutual information, and modularity perspective. We further quantify the accuracy and conflict of extracted logic programs. We demonstrate the effectiveness of the proposed method with extensive experimental analysis across various types of compact network architectures on a series of end-to-end policy learning tasks.

Acknowledgments

This work was partially supported by Capgemini Engineering. This research was also sponsored by the United States Air Force Research Laboratory and the United States Air Force Artificial Intelligence Accelerator and was accomplished under Cooperative Agreement Number FA8750-19-2-1000. The views and conclusions contained in this document are those of the authors and should not be interpreted as representing the official policies, either expressed or implied, of the United States Air Force or the U.S. Government. The U.S. Government is authorized to reproduce and distribute reprints for Government purposes notwithstanding any copyright notation herein.

References

- D. Alvarez Melis and T. Jaakkola. Towards robust interpretability with self-explaining neural networks. *Advances in neural information processing systems*, 31, 2018.
- A. Amini, T.-H. Wang, I. Gilitschenski, W. Schwarting, Z. Liu, S. Han, S. Karaman, and D. Rus. Vista 2.0: An open, data-driven simulator for multimodal sensing and policy learning for autonomous vehicles. In *2022 International Conference on Robotics and Automation (ICRA)*. IEEE, 2022.
- Z. Babaiee, R. Hasani, M. Lechner, D. Rus, and R. Grosu. On-Off Center-Surround Receptive Fields for Accurate and Robust Image Classification. In *Proceedings of the 38th International Conference on Machine Learning*, pages 478–489. PMLR, July 2021. URL <https://proceedings.mlr.press/v139/babaiee21a.html>. ISSN: 2640-3498.
- Z. Babaiee, L. Liebenwein, R. Hasani, D. Rus, and R. Grosu. End-to-End Sensitivity-Based Filter Pruning. *arXiv preprint arXiv:2204.07412*, 2022.
- Y. Bengio, A. Courville, and P. Vincent. Representation learning: A review and new perspectives. *IEEE transactions on pattern analysis and machine intelligence*, 35(8):1798–1828, 2013.
- G. Brockman, V. Cheung, L. Pettersson, J. Schneider, J. Schulman, J. Tang, and W. Zaremba. Openai gym. *arXiv preprint arXiv:1606.01540*, 2016.
- A. Brunnbauer, L. Berducci, A. Brandstätter, M. Lechner, R. Hasani, D. Rus, and R. Grosu. Latent Imagination Facilitates Zero-Shot Transfer in Autonomous Racing. In *2022 International Conference on Robotics and Automation (ICRA)*, pages 7513–7520, May 2022. doi: 10.1109/ICRA46639.2022.9811650.

- R. T. Chen, X. Li, R. B. Grosse, and D. K. Duvenaud. Isolating sources of disentanglement in variational autoencoders. *Advances in neural information processing systems*, 31, 2018a.
- R. T. Chen, Y. Rubanova, J. Bettencourt, and D. K. Duvenaud. Neural ordinary differential equations. *Advances in neural information processing systems*, 31, 2018b.
- K. Cho, B. Van Merriënboer, D. Bahdanau, and Y. Bengio. On the properties of neural machine translation: Encoder-decoder approaches. *arXiv preprint arXiv:1409.1259*, 2014.
- C. Chyung, M. Tsang, and Y. Liu. Extracting interpretable concept-based decision trees from cnns. *arXiv preprint arXiv:1906.04664*, 2019.
- J. DelPreto, A. F. Salazar-Gomez, S. Gil, R. Hasani, F. H. Guenther, and D. Rus. Plug-and-play supervisory control using muscle and brain signals for real-time gesture and error detection. *Autonomous Robots*, 44(7): 1303–1322, 2020. Publisher: Springer.
- J. Frankle and M. Carbin. The lottery ticket hypothesis: Finding sparse, trainable neural networks. In *International Conference on Learning Representations*, 2018.
- S. A. Gruenbacher, M. Lechner, R. Hasani, D. Rus, T. A. Henzinger, S. A. Smolka, and R. Grosu. GoTube: Scalable Statistical Verification of Continuous-Depth Models. *Proceedings of the AAAI Conference on Artificial Intelligence*, 36(6):6755–6764, June 2022. ISSN 2374-3468. doi: 10.1609/aaai.v36i6.20631. URL <https://ojs.aaai.org/index.php/AAAI/article/view/20631>. Number: 6.
- S. Grunbacher, R. Hasani, M. Lechner, J. Cyranka, S. A. Smolka, and R. Grosu. On the Verification of Neural ODEs with Stochastic Guarantees. *Proceedings of the AAAI Conference on Artificial Intelligence*, 35(13): 11525–11535, May 2021. ISSN 2374-3468. doi: 10.1609/aaai.v35i13.17372. URL <https://ojs.aaai.org/index.php/AAAI/article/view/17372>. Number: 13.
- R. Hasani. *Interpretable recurrent neural networks in continuous-time control environments*. Thesis, Wien, 2020. URL <https://repositum.tuwien.at/handle/20.500.12708/1068>. Accepted: 2020-06-27T19:05:20Z.
- R. Hasani, A. Amini, M. Lechner, F. Naser, R. Grosu, and D. Rus. Response characterization for auditing cell dynamics in long short-term memory networks. In *2019 International Joint Conference on Neural Networks (IJCNN)*, pages 1–8. IEEE, 2019.
- R. Hasani, M. Lechner, A. Amini, D. Rus, and R. Grosu. A natural lottery ticket winner: Reinforcement learning with ordinary neural circuits. In *International Conference on Machine Learning*, pages 4082–4093. PMLR, 2020.
- R. Hasani, M. Lechner, A. Amini, L. Liebenwein, M. Tschaikowski, G. Teschl, and D. Rus. Closed-form continuous-depth models. *arXiv preprint arXiv:2106.13898*, 2021a.
- R. Hasani, M. Lechner, A. Amini, D. Rus, and R. Grosu. Liquid Time-constant Networks. *Proceedings of the AAAI Conference on Artificial Intelligence*, 35(9):7657–7666, May 2021b. doi: 10.1609/aaai.v35i9.16936. URL <https://ojs.aaai.org/index.php/AAAI/article/view/16936>.
- R. Hasani, M. Lechner, T.-H. Wang, M. Chahine, A. Amini, and D. Rus. Liquid Structural State-Space Models, Sept. 2022. URL <http://arxiv.org/abs/2209.12951>. arXiv:2209.12951 [cs].

- R. M. Hasani, D. Haerle, and R. Grosu. Efficient modeling of complex Analog integrated circuits using neural networks. In *2016 12th Conference on Ph.D. Research in Microelectronics and Electronics (PRIME)*, pages 1–4, June 2016. doi: 10.1109/PRIME.2016.7519486.
- R. M. Hasani, D. Haerle, C. F. Baumgartner, A. R. Lomuscio, and R. Grosu. Compositional neural-network modeling of complex analog circuits. In *2017 International Joint Conference on Neural Networks (IJCNN)*, pages 2235–2242. IEEE, 2017.
- S. Hochreiter and J. Schmidhuber. Long short-term memory. *Neural computation*, 9(8):1735–1780, 1997.
- M. Lechner and R. Hasani. Learning Long-Term Dependencies in Irregularly-Sampled Time Series, Dec. 2020. URL <http://arxiv.org/abs/2006.04418>. arXiv:2006.04418 [cs, stat].
- M. Lechner, R. Hasani, M. Zimmer, T. A. Henzinger, and R. Grosu. Designing worm-inspired neural networks for interpretable robotic control. In *2019 International Conference on Robotics and Automation (ICRA)*, pages 87–94. IEEE, 2019.
- M. Lechner, R. Hasani, A. Amini, T. A. Henzinger, D. Rus, and R. Grosu. Neural circuit policies enabling auditable autonomy. *Nature Machine Intelligence*, 2(10):642–652, 2020a.
- M. Lechner, R. Hasani, D. Rus, and R. Grosu. Gershgorin loss stabilizes the recurrent neural network compartment of an end-to-end robot learning scheme. In *2020 IEEE International Conference on Robotics and Automation (ICRA)*, pages 5446–5452. IEEE, 2020b.
- M. Lechner, R. Hasani, R. Grosu, D. Rus, and T. A. Henzinger. Adversarial Training is Not Ready for Robot Learning. In *2021 IEEE International Conference on Robotics and Automation (ICRA)*, pages 4140–4147, May 2021. doi: 10.1109/ICRA48506.2021.9561036. ISSN: 2577-087X.
- M. Lechner, R. Hasani, Z. Babaiee, R. Grosu, D. Rus, T. A. Henzinger, and S. Hochreiter. Entangled Residual Mappings. *arXiv preprint arXiv:2206.01261*, 2022.
- L. Liebenwein, C. Baykal, B. Carter, D. Gifford, and D. Rus. Lost in pruning: The effects of pruning neural networks beyond test accuracy. *Proceedings of Machine Learning and Systems*, 3:93–138, 2021a.
- L. Liebenwein, R. Hasani, A. Amini, and D. Rus. Sparse flows: Pruning continuous-depth models. *Advances in Neural Information Processing Systems*, 34, 2021b.
- F. Locatello, S. Bauer, M. Lucic, G. Raetsch, S. Gelly, B. Schölkopf, and O. Bachem. Challenging common assumptions in the unsupervised learning of disentangled representations. In *international conference on machine learning*, pages 4114–4124. PMLR, 2019.
- J. Peters, D. Janzing, and B. Schölkopf. *Elements of causal inference: foundations and learning algorithms*. The MIT Press, 2017.
- K. Ridgeway and M. C. Mozer. Learning deep disentangled embeddings with the f-statistic loss. *Advances in neural information processing systems*, 31, 2018.
- Y. Rubanova, R. T. Chen, and D. K. Duvenaud. Latent ordinary differential equations for irregularly-sampled time series. *Advances in neural information processing systems*, 32, 2019.

- N. Schaaf, M. Huber, and J. Maucher. Enhancing decision tree based interpretation of deep neural networks through 11-orthogonal regularization. In *2019 18th IEEE International Conference On Machine Learning And Applications (ICMLA)*, pages 42–49, 2019. doi: 10.1109/ICMLA.2019.00016.
- J. Schmidhuber. Learning factorial codes by predictability minimization. *Neural computation*, 4(6):863–879, 1992.
- B. Schölkopf, F. Locatello, S. Bauer, N. R. Ke, N. Kalchbrenner, A. Goyal, and Y. Bengio. Toward causal representation learning. *Proceedings of the IEEE*, 109(5):612–634, 2021.
- J. Schulman, F. Wolski, P. Dhariwal, A. Radford, and O. Klimov. Proximal policy optimization algorithms. *arXiv preprint arXiv:1707.06347*, 2017.
- S. Sietzen, M. Lechner, J. Borowski, R. Hasani, and M. Waldner. Interactive Analysis of CNN Robustness. *Computer Graphics Forum*, 40(7):253–264, 2021. ISSN 1467-8659. doi: 10.1111/cgf.14418. URL <https://onlinelibrary.wiley.com/doi/abs/10.1111/cgf.14418>. eprint: <https://onlinelibrary.wiley.com/doi/pdf/10.1111/cgf.14418>.
- B. A. Toms, E. A. Barnes, and I. Ebert-Uphoff. Physically interpretable neural networks for the geosciences: Applications to earth system variability. *Journal of Advances in Modeling Earth Systems*, 12(9):e2019MS002002, 2020.
- T. Ueno and Q. Zhao. Interpretation of deep neural networks based on decision trees. In *2018 IEEE 16th Intl Conf on Dependable, Autonomic and Secure Computing, 16th Intl Conf on Pervasive Intelligence and Computing*, pages 256–261, 2018. doi: 10.1109/DASC/PiCom/DataCom/CyberSciTec.2018.00052.
- C. Vorbach, R. Hasani, A. Amini, M. Lechner, and D. Rus. Causal navigation by continuous-time neural networks. *Advances in Neural Information Processing Systems*, 34, 2021.
- A. Wan, L. Dunlap, D. Ho, J. Yin, S. Lee, S. Petryk, S. A. Bargal, and J. E. Gonzalez. {NBDT}: Neural-backed decision tree. In *International Conference on Learning Representations*, 2021. URL <https://openreview.net/forum?id=mCLVeEplNE>.
- M. Wu, S. Parbhoo, M. C. Hughes, V. Roth, and F. Doshi-Velez. Optimizing for interpretability in deep neural networks with tree regularization. *Journal of Artificial Intelligence Research*, 72:1–37, 2021.
- W. Xiao, R. Hasani, X. Li, and D. Rus. BarrierNet: A safety-guaranteed layer for neural networks. *arXiv preprint arXiv:2111.11277*, 2021.
- W. Xiao, T.-H. Wang, M. Chahine, A. Amini, R. Hasani, and D. Rus. Differentiable Control Barrier Functions for Vision-based End-to-End Autonomous Driving. *arXiv preprint arXiv:2203.02401*, 2022a.
- W. Xiao, T.-H. Wang, R. Hasani, M. Lechner, and D. Rus. On the Forward Invariance of Neural ODEs, Oct. 2022b. URL <http://arxiv.org/abs/2210.04763>. arXiv:2210.04763 [cs, eess].
- Q. Zhang, Y. N. Wu, and S.-C. Zhu. Interpretable convolutional neural networks. In *Proceedings of the IEEE conference on computer vision and pattern recognition*, pages 8827–8836, 2018.
- Q. Zhang, Y. Yang, H. Ma, and Y. N. Wu. Interpreting cnns via decision trees. In *Proceedings of the IEEE/CVF conference on computer vision and pattern recognition*, pages 6261–6270, 2019.
- Y. Zhang, P. Tiño, A. Leonardis, and K. Tang. A survey on neural network interpretability. *IEEE Transactions on Emerging Topics in Computational Intelligence*, 2021.

Appendix

S1. Calibration Of Mutual Information

Proof. In the main paper, we adapting Mutual Information Gap (MIG) (Chen et al., 2018a) to our framework as,

$$\frac{1}{K} \sum_{k=1}^K \frac{1}{H[\mathcal{P}_k]} \left(I[z^{i^*}; \mathcal{P}_k] - \max_{j \neq i^*} I[z^j; \mathcal{P}_k] - I[z^j; \mathcal{P}_k; \mathcal{P}_{kj}] \right)$$

and Modularity score (Ridgeway and Mozer, 2018) as,

$$\frac{1}{\mathcal{I}} \sum_{i \in \mathcal{I}} 1 - \frac{\sum_{k \neq k^*} (I[z^i; \mathcal{P}_k] - I[z^i; \mathcal{P}_k; \mathcal{P}_{k^*}])^2}{(K-1)I[z^i; \mathcal{P}_{k^*}]^2}$$

Both involve the computation of $I[z^j; \mathcal{P}_k; \mathcal{P}_{kj}]$. Without loss of generality for both cases (and with the notation of MIG), we simplify the calibration term for $j \neq i^*$ as follows,

$$\begin{aligned} & I[z^j; \mathcal{P}_k] - I[z^j; \mathcal{P}_k; \mathcal{P}_{kj}] \\ &= I[z^j; \mathcal{P}_k] - (I[z^j; \mathcal{P}_k] - I[z^j; \mathcal{P}_k | \mathcal{P}_{kj}]) \\ &= I[z^j; \mathcal{P}_k | \mathcal{P}_{kj}] \\ &= I[z^j; \mathcal{P}_k] + H[\mathcal{P}_{kj} | z^j] + H[\mathcal{P}_{kj} | \mathcal{P}_k] - H[\mathcal{P}_{kj} | z^j, \mathcal{P}_k] - H[\mathcal{P}_{kj}] \\ &= I[z^j; \mathcal{P}_k] - (H[\mathcal{P}_{kj}] - H[\mathcal{P}_{kj} | \mathcal{P}_k]) + (H[\mathcal{P}_{kj} | z^j] - H[\mathcal{P}_{kj} | z^j, \mathcal{P}_k]) \\ &= I[z^j; \mathcal{P}_k] - I[\mathcal{P}_k; \mathcal{P}_{kj}] + I[\mathcal{P}_{kj} | z^j; \mathcal{P}_k] \\ &\geq \max(0, I[z^j; \mathcal{P}_k] - I[\mathcal{P}_k; \mathcal{P}_{kj}]) \end{aligned}$$

Most steps simply follow identities of mutual information and entropy. The last step requires access to the conditional distribution of random variable $(\mathcal{P}_{kj} | z^j)$, which is normally inaccessible. Hence, we introduce an approximation that serves as a lower bound for the calibrated mutual information in our implementation. \square

S2. Implementation Details

S2.1. Classical Control (Pendulum)

Network Architecture. With 3-dimensional observation space and 1-dimensional action space, we use the following network architecture for compact neural policies.

- *FCs*: a $3 \rightarrow 10 \rightarrow 4 \rightarrow 1$ fully-connected network with *tanh* activation.
- *GRU*: a $3 \rightarrow 10$ fully-connected network with *tanh* activation followed by GRU with cell size of 4, outputting a 1-dimensional action.
- *LSTM*: a $3 \rightarrow 10$ fully-connected network with *tanh* activation followed by LSTM with hidden size of 4, outputting a 1-dimensional action. Note that this effectively gives 8 cells by considering hidden and cell states.
- *ODE-RNN*: a $3 \rightarrow 10$ fully-connected network with *tanh* activation followed by a neural ODE with recurrent component both of size 4, outputting a 1-dimensional action.

- *CfC*: with backbone layer = 1, backbone unit = 10, backbone activation *silu*, hidden size = 4 without gate and mixed memory, outputting a 1-dimensional action.
- *NCP*: with 3 sensory neurons, 10 interneuron, 4 command neurons, 1 motor neuron, 4 output sensory synapses, 3 output inter-synapses, 2 recurrent command synapse, 3 motor synapses.

For all policies, we use a $3 \rightarrow 64 \rightarrow 64 \rightarrow 1$ fully-connected networks with *tanh* activation as value function. We interpret the layer of size 4 for each policy.

Training details. We use PPO with the following parameters for all models. Learning rate is 0.0003. Train batch size (of an epoch) is 512. Mini-batch size is 64. Number of iteration within a batch is 6. Value function clip parameter is 10.0. Discount factor of the MDP is 0.95. Generalized advantage estimation parameter is 0.95. Initial coefficient of KL divergence is 0.2. Clip parameter is 0.3. Training halts if reaching target average episode reward 150. Maximal training steps is 1M.

Interpreter details. For the decision tree T_{ϕ^i} , we set minimum number of samples required to be at a leaf node as 10% of the training data, criterion of a split as mean squared error with Friedman’s improvement score, the maximum depth of the tree as 3, complexity parameter used for minimal cost-complexity pruning as 0.003; we use scikit-learn implementation of CART (Classification and Regression Trees). For simplicity, we use another decision tree as decision path classifier q_{ϕ^i} with maximal depth of tree as 3, minimum number of samples in a leaf node as 1% of data, complexity parameter for pruning as 0.01, criterion as Gini impurity. The state grounding \mathcal{S} of the interpreter $f_{\mathcal{S}}^i$ is $\{\theta, \dot{\theta}\}$, where θ is joint angle and $\dot{\theta}$ is joint angular velocity.

S2.2. Locomotion (HalfCheetah)

Network Architecture. With 17-dimensional observation space and 6-dimensional action space, we first use feature extractors of a shared architecture as a $17 \rightarrow 256$ fully-connected network, which then output features to compact neural policies with the following architectures,

- *FCs*: a $256 \rightarrow 20 \rightarrow 10 \rightarrow 6$ fully-connected network with *tanh* activation.
- *GRU*: a $256 \rightarrow 20$ fully-connected network with *tanh* activation followed by GRU with cell size of 10, outputting a 6-dimensional action.
- *LSTM*: a $256 \rightarrow 20$ fully-connected network with *tanh* activation followed by LSTM with hidden size of 10, outputting a 6-dimensional action. Note that this effectively gives 20 cells by considering hidden and cell states.
- *ODE-RNN*: a $256 \rightarrow 20$ fully-connected network with *tanh* activation followed by a neural ODE with recurrent component both of size 10, outputting a 6-dimensional action.
- *CfC*: with backbone layer = 1, backbone unit = 20, backbone activation *silu*, hidden size = 10 without gate and mixed memory.
- *NCP*: with 256 sensory neurons, 20 interneuron, 10 command neurons, 6 motor neuron, 4 output sensory synapses, 5 output inter-synapses, 6 recurrent command synapse, 4 input motor synapses.

For all policies, we use a $17 \rightarrow 256 \rightarrow 256 \rightarrow 1$ fully-connected networks with *tanh* activation as value function. We interpret the layer of size 10 for each policy.

Training details. We use PPO with the following parameters for all models. Learning rate is 0.0003. Train batch size (of an epoch) is 65536. Mini-batch size is 4096. Number of iteration within a batch is 32. Value function coefficient is 10.0. Discount factor of the MDP is 0.99. Generalized advantage estimation parameter is

0.95. Initial coefficient of KL divergence is 1.0. Clip parameter is 0.2. Gradient norm clip is 0.5. Training halts if reaching target average episode reward -500 . Maximal training steps is 12M.

Interpreter details. For the decision tree T_{θ^i} , we set minimum number of samples required to be at a leaf node as 10% of the training data, criterion of a split as mean squared error with Friedman’s improvement score, the maximum depth of the tree as 3, complexity parameter used for minimal cost-complexity pruning as 0.001; we use scikit-learn implementation of CART (Classification and Regression Trees). For simplicity, we use another decision tree as decision path classifier q_{ϕ^i} with maximal depth of tree as 3, minimum number of samples in a leaf node as 1% of data, complexity parameter for pruning as 0.01, criterion as Gini impurity. The state grounding \mathcal{S} of the interpreter $f_{\mathcal{S}}^i$ is $\{h_R, \theta_R, \theta_{T,B}, \theta_{S,B}, \theta_{F,B}, \theta_{T,F}, \theta_{S,F}, \theta_{F,F}, \dot{x}_R, \dot{h}_R, \dot{\theta}_R, \dot{\theta}_{T,B}, \dot{\theta}_{S,B}, \dot{\theta}_{F,B}, \dot{\theta}_{T,F}, \dot{\theta}_{S,F}, \dot{\theta}_{F,F}\}$, where h_R, \dot{h}_R are position and velocity of z-coordinate of the front tip, $\theta_R, \dot{\theta}_R$ are angle and angular velocity of the front tip, $\theta_{T,B}, \dot{\theta}_{T,B}$ are angle and angular velocity of the thigh in the back, $\theta_{S,B}, \dot{\theta}_{S,B}$ are angle and angular velocity of the shin in the back, $\theta_{F,B}, \dot{\theta}_{F,B}$ are angle and angular velocity of the foot in the back, $\theta_{T,T}, \dot{\theta}_{T,T}$ are angle and angular velocity of the thigh in the front, $\theta_{S,T}, \dot{\theta}_{S,T}$ are angle and angular velocity of the shin in the front, $\theta_{F,T}, \dot{\theta}_{F,T}$ are angle and angular velocity of the foot in the front, \dot{x}_R is the velocity of x-coordinate of the front tip.

S2.3. End-to-end visual servoing (Image-based Driving)

Network Architecture. With image observation space of size (200, 320, 3) and 2-dimensional action space, we first use feature extractors of a shared architecture as a convolutional neural network (CNN) in Table S1, which then output features to compact neural policies with the following architectures,

- *FCs*: a 1280 \rightarrow 20 \rightarrow 8 \rightarrow 2 fully-connected network with *tanh* activation.
- *GRU*: a 1280 \rightarrow 20 fully-connected network with *tanh* activation followed by GRU with cell size of 8, outputting a 2-dimensional action.
- *LSTM*: a 1280 \rightarrow 20 fully-connected network with *tanh* activation followed by LSTM with hidden size of 8, outputting a 2-dimensional action. Note that this effectively gives 20 cells by considering hidden and cell states.
- *ODE-RNN*: a 1280 \rightarrow 20 fully-connected network with *tanh* activation followed by a neural ODE with recurrent component both of size 8, outputting a 2-dimensional action.
- *CfC*: with backbone layer = 1, backbone unit = 20, backbone activation *silu*, hidden size = 8 without gate and mixed memory.
- *NCP*: with 1280 sensory neurons, 20 interneuron, 8 command neurons, 2 motor neuron, 4 output sensory synapses, 5 output inter-synapses, 6 recurrent command synapse, 4 input motor synapses.

Training details. Batch size is 64. Sequence size is 10. Learning rate is 0.001. Number of epochs is 10. We perform data augmentation on RGB images with randomized gamma of range [0.5, 1.5], brightness of range [0.5, 1.5], contrast of range [0.7, 1.3], saturation of range [0.5, 1.5].

Interpreter details. For the decision tree T_{θ^i} , we set minimum number of samples required to be at a leaf node as 10% of the training data, criterion of a split as mean squared error with Friedman’s improvement score, the maximum depth of the tree as 3, complexity parameter used for minimal cost-complexity pruning as 0.003; we use scikit-learn implementation of CART (Classification and Regression Trees). For simplicity, we use another decision tree as decision path classifier q_{ϕ^i} with maximal depth of tree as 3, minimum number of samples in a leaf node as 1% of data, complexity parameter for pruning as 0.01, criterion as Gini impurity. The state grounding \mathcal{S} of the interpreter $f_{\mathcal{S}}^i$ is $\{v, \delta, d, \Delta l, \mu, \kappa\}$, where v is vehicle speed, δ is heading, d is lateral deviation from the lane center, Δl is longitudinal deviation from the lane center, μ is local heading error with respect to the lane center, κ is road curvature.

Layer	Hyperparameters
Conv2d	(3, 24, 5, 2, 2)
GroupNorm2d	(16, 1e-5)
ELU	-
Dropout	0.3
Conv2d	(24, 36, 5, 2, 2)
GroupNorm2d	(16, 1e-5)
ELU	-
Dropout	0.3
Conv2d	(36, 48, 3, 2, 1)
GroupNorm2d	(16, 1e-5)
ELU	-
Dropout	0.3
Conv2d	(48, 64, 3, 1, 1)
GroupNorm2d	(16, 1e-5)
ELU	-
Dropout	0.3
Conv2d	(64, 64, 3, 1, 1)
AdaptiveAvgPool2d	reduce height dimension

Table S1: Network architecture of CNN feature extractor for end-to-end visual servoing. Hyperparameters for *Conv2d* are input channel, output channel, kernel size, stride, and padding; for *GroupNorm2d*, they are group size and epsilon; for *Dropout*, it is drop probability.

S3. Robustness Analysis

We propose to study the interpretability of neural policies through decision trees and present several quantitative measures of interpretability by analyzing various properties on top of neuron responses and corresponding decision trees, including *Neural-Response Variance*, *Mutual Information Gap*, *Modularity*, *Decision Path Accuracy*, and *Logic Conflict*. However, the extracted decision trees may differ across different configurations. Hence, to validate the robustness of the proposed metrics to hyperparameters, we compute all metrics with different decision tree parameters in classical control environment (Pendulum). We report the averaged results with 5 random seeds in Table S2 (*Neural-Response Variance*), Table S3 (*Mutal Information Gap*), Table S4 (*Modularity*), Table S5 (*Decision Path Accuracy*), Table S6 (*Logic Conflict*). Most metrics (variance, MI-gap, decision path accuracy, logic conflict) yield consistent top-1 results and agree with similar rankings among network architectures, except for modularity that is slightly less robust against hyperparameters yet still consistent in the top-3 set of models. This results demonstrate the reliability of the proposed interpretability analysis for neural policies.

S4. Interpretation Of Driving Maneuver

In Figure 3, we describe interpretations similar to classical control (for a neuron in NCP). While the state space of driving is higher dimensional (5 with bicycle model for lane following), states of interest only include local

Table S2: Robustness to hyperparameters for *Neural-Response Variance*. The results are averaged across 5 random seeds in classical control (Pendulum).

[Variance] Network Architecture	FCs	GRU	LSTM	ODE-RNN	CfC	NCP	
Cost Complexity Pruning	0.001	0.0232	0.0304	0.0209	0.0266	0.0254	0.0207
	0.003	0.0242	0.0329	0.0216	0.0287	0.0272	0.0240
	0.01	0.0261	0.0371	0.0221	0.0315	0.0267	0.0305
Minimal Leaf Sample Ratio	0.01	0.0154	0.0261	0.0138	0.0193	0.0189	0.0186
	0.1	0.0242	0.0329	0.0216	0.0287	0.0272	0.0240
	0.2	0.0334	0.0387	0.0284	0.0354	0.0295	0.0285

Table S3: Robustness to hyperparameters for *Mutual Information Gap*. The results are averaged across 5 random seeds in classical control (Pendulum).

[MI-Gap] Network Architecture	FCs	GRU	LSTM	ODE-RNN	CfC	NCP	
Cost Complexity Pruning	0.001	0.0284	0.2686	0.2026	0.2891	0.2544	0.3403
	0.003	0.3008	0.2764	0.2303	0.3062	0.2892	0.3653
	0.01	0.3482	0.3065	0.2547	0.3142	0.3567	0.3664
Minimal Leaf Sample Ratio	0.01	0.2824	0.2632	0.2040	0.2819	0.2433	0.3456
	0.1	0.3008	0.2764	0.2303	0.3062	0.2892	0.3653
	0.2	0.3798	0.3387	0.2528	0.3168	0.3342	0.3429

heading error μ and lateral deviation from the lane center d in lane following task. We compute the statistics and plot neuron response and closed-loop dynamics in the d - μ phase portrait. This specific neuron develops more fine-grained control for situations when the vehicle is on the right of the lane center, as shown in Figure 3(a). We further show front-view images retrieved based on neuron response in Figure 3(b).

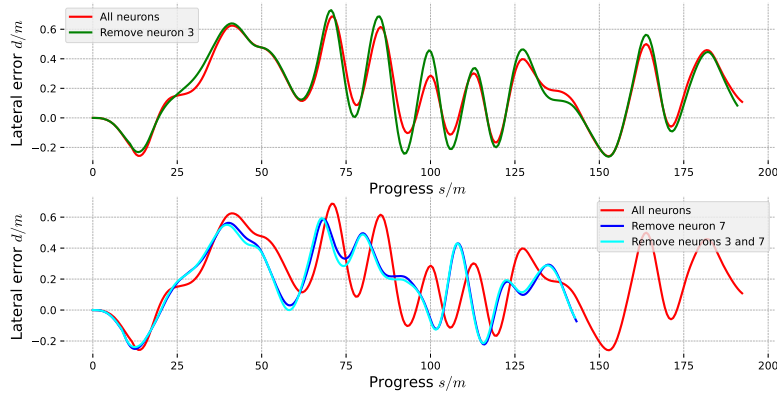

Fig. S1: Driving profile when removing neurons according to decision tree interpretation.

Table S4: Robustness to hyperparameters for *Modularity*. The results are averaged across 5 random seeds in classical control (Pendulum).

[Modularity] Network Architecture	FCs	GRU	LSTM	ODE-RNN	CfC	NCP	
Cost Complexity Pruning	0.001	0.9519	0.9558	0.9327	0.9485	0.9228	0.9438
	0.003	0.9471	0.9550	0.9402	0.9486	0.9116	0.9551
	0.01	0.9532	0.9598	0.9445	0.9487	0.8970	0.9593
Minimal Leaf Sample Ratio	0.01	0.9638	0.9702	0.9547	0.9630	0.9333	0.9651
	0.1	0.9471	0.9550	0.9402	0.9486	0.9116	0.9551
	0.2	0.9475	0.9372	0.9197	0.9404	0.8755	0.9301

Table S5: Robustness to hyperparameters for *Decision Path Accuracy*. The results are averaged across 5 random seeds in classical control (Pendulum).

[Decision Path Accuracy] Network Architecture	FCs	GRU	LSTM	ODE-RNN	CfC	NCP	
Cost Complexity Pruning	0.001	0.2815	0.2415	0.2195	0.2904	0.2250	0.4294
	0.003	0.3015	0.2504	0.2392	0.2980	0.2509	0.4726
	0.01	0.3074	0.3330	0.3161	0.3707	0.2864	0.4390
Minimal Leaf Sample Ratio	0.01	0.2950	0.2637	0.2270	0.2574	0.2452	0.4287
	0.1	0.3015	0.2504	0.2392	0.2980	0.2509	0.4726
	0.2	0.3572	0.3587	0.2794	0.3322	0.2784	0.4684

S5. Logic Program from Decision Trees

Here we show the corresponding logic program of the finite set of decision path $\{r(\mathcal{P}_k^i)\}_{k=1}^{K^i}$ for every interpreted neuron in all network architectures. The symbols used in the logic program follow the state grounding definition in Section S2.

In classical control (Pendulum), the extracted logic program are shown in Table S7 (FC), Table S8 (GRU), Table S9 (LSTM), Table S10 (ODE-RNN), Table S11 (CfC), Table S12 (NCP).

In locomotion (HalfCheetah), the extracted logic program are shown in Table S13 (FC), Table S14 (GRU), Table S15 (LSTM), Table S16 (ODE-RNN), Table S17 (CfC), Table S18 (NCP).

In end-to-end visual servoing (Image-based Driving), the extracted logic program are shown in Table S19 (FC), Table S20 (GRU), Table S21 (LSTM), Table S22 (ODE-RNN), Table S23 (CfC), Table S24 (NCP).

In a logic program, "conflict" indicates there are conflict between predicates within the logic program as elaborated in Section 4.3.

Table S6: Robustness to hyperparameters for *Logic Conflict*. The results are averaged across 5 random seeds in classical control (Pendulum).

[Logic Conflict] Network Architecture		FCs	GRU	LSTM	ODE-RNN	CfC	NCP
Cost Complexity Pruning	0.001	0.2451	0.3348	0.5240	0.2641	0.2048	0.3159
	0.003	0.2104	0.2832	0.5072	0.2506	0.1556	0.2026
	0.01	0.1766	0.1877	0.4325	0.1401	0.1121	0.2924
Minimal Leaf Sample Ratio	0.01	0.2672	0.4298	0.6791	0.3575	0.2654	0.2607
	0.1	0.2104	0.2832	0.5072	0.2506	0.1556	0.2026
	0.2	0.1796	0.1664	0.3842	0.2001	0.1089	0.1111

Table S7: Logic program of FC in classical control (Pendulum).

Model	Neuron	Logic Program
FC	0	0: $(\dot{\theta} \leq 0.69) \wedge (\theta \leq -2.18)$ 1: $(\dot{\theta} > 0.69) \wedge (\theta \leq -2.18)$ 2: (conflict) 3: $(\theta \leq 2.41) \wedge (\theta > -2.18)$ 4: $(\theta > 2.41)$
	1	0: $(\dot{\theta} \leq -1.16) \wedge (\theta \leq -0.34)$ 1: $(\dot{\theta} \leq 1.73) \wedge (\dot{\theta} > -1.16) \wedge (\theta \leq -0.34)$ 2: $(\dot{\theta} > 1.73) \wedge (\theta \leq -0.34)$ 3: $(\theta \leq 2.03) \wedge (\theta > -0.34)$ 4: $(\theta \leq 2.62) \wedge (\theta > 2.03)$ 5: $(\theta > 2.62)$
	2	0: $(\dot{\theta} \leq -1.54) \wedge (\theta \leq -1.68)$ 1: $(\dot{\theta} \leq 1.47) \wedge (\dot{\theta} > -1.54) \wedge (\theta \leq -1.68)$ 2: $(\dot{\theta} > 1.47) \wedge (\theta \leq -1.68)$ 3: (conflict) 4: $(\theta \leq 2.48) \wedge (\theta > -1.68)$ 5: $(\theta > 2.48)$
	3	0: $(\theta \leq -2.76)$ 1: (conflict) 2: $(\theta \leq 0.05) \wedge (\theta > -2.76)$ 3: $(\theta > 0.05)$

Table S8: Logic program of GRU in classical control (Pendulum).

Model	Neuron	Logic Program
GRU	0	0: $(\theta \leq -0.06)$ 1: (conflict) 2: $(\dot{\theta} \leq -0.30) \wedge (\theta > -0.06)$ 3: $(\dot{\theta} \leq 1.75) \wedge (\dot{\theta} > -0.30) \wedge (\theta > -0.06)$ 4: $(\dot{\theta} > 1.75) \wedge (\theta > -0.06)$
	1	0: $(\dot{\theta} \leq -2.30) \wedge (\theta \leq -1.27)$ 1: $(\dot{\theta} \leq 1.83) \wedge (\dot{\theta} > -2.30) \wedge (\theta \leq -1.27)$ 2: $(\dot{\theta} \leq -0.37) \wedge (\theta > -1.27)$ 3: $(\dot{\theta} \leq 1.83) \wedge (\dot{\theta} > -0.37) \wedge (\theta > -1.27)$ 4: $(\dot{\theta} \leq 3.10) \wedge (\dot{\theta} > 1.83)$ 5: $(\dot{\theta} > 3.10)$
	2	0: $(\dot{\theta} \leq -0.11) \wedge (\theta \leq -0.05)$ 1: $(\dot{\theta} \leq -0.11) \wedge (\theta > -0.05)$ 2: (conflict) $\wedge (\theta > -0.05)$ 3: $(\dot{\theta} > -0.11) \wedge (\theta \leq -2.09)$ 4: $(\dot{\theta} > -0.11) \wedge (\theta \leq 0.41) \wedge (\theta > -2.09)$ 5: $(\dot{\theta} \leq 1.61) \wedge (\dot{\theta} > -0.11) \wedge (\theta > 0.41)$ 6: $(\dot{\theta} > 1.61) \wedge (\theta > 0.41)$
	3	0: $(\theta \leq -2.61)$ 1: $(\dot{\theta} \leq 2.44) \wedge (\theta \leq 0.21) \wedge (\theta > -2.61)$ 2: $(\dot{\theta} > 2.44) \wedge (\theta \leq 0.21) \wedge (\theta > -2.61)$ 3: $(\dot{\theta} \leq -1.76) \wedge (\theta > 0.21)$ 4: $(\dot{\theta} \leq 0.39) \wedge (\dot{\theta} > -1.76) \wedge (\theta > 0.21)$ 5: $(\dot{\theta} > 0.39) \wedge (\theta > 0.21)$

Table S9: Logic program of LSTM in classical control (Pendulum).

Model	Neuron	Logic Program
LSTM	0	0: $(\theta \leq -2.16)$ 1: (conflict) 2: $(\theta \leq 0.01) \wedge (\theta > -2.16)$ 3: $(\dot{\theta} \leq 0.48) \wedge (\theta > 0.01)$ 4: $(\dot{\theta} \leq 3.00) \wedge (\dot{\theta} > 0.48) \wedge (\theta > 0.01)$ 5: $(\dot{\theta} > 3.00) \wedge (\theta > 0.01)$
	1	0: $(\dot{\theta} \leq -2.57)$ 1: (conflict) 2: $(\dot{\theta} > -2.57) \wedge (\theta \leq 0.35)$ 3: $(\dot{\theta} > -2.57) \wedge (\theta \leq 2.03) \wedge (\theta > 0.35)$ 4: $(\dot{\theta} > -2.57) \wedge (\theta > 2.03)$
	2	0: $(\dot{\theta} \leq 4.79) \wedge (\theta \leq -2.31)$ 1: $(\dot{\theta} \leq 4.79) \wedge (\theta \leq 1.72) \wedge (\theta > -2.31)$ 2: $(\dot{\theta} \leq -3.13) \wedge (\theta > 1.72)$ 3: $(\dot{\theta} \leq 4.79) \wedge (\dot{\theta} > -3.13) \wedge (\theta > 1.72)$ 4: $(\dot{\theta} > 4.79)$
	3	0: $(\theta \leq -2.32)$ 1: $(\theta \leq 0.93) \wedge (\theta > -2.32)$ 2: $(\dot{\theta} \leq -3.98) \wedge (\theta > 0.93)$ 3: $(\dot{\theta} > -3.98) \wedge (\theta \leq 2.04) \wedge (\theta > 0.93)$ 4: $(\dot{\theta} > -3.98) \wedge (\theta > 2.04)$

Table S10: Logic program of ODE-RNN in classical control (Pendulum).

Model	Neuron	Logic Program
ODE-RNN	0	0: $(\dot{\theta} \leq -1.48) \wedge (\theta \leq -0.02)$ 1: $(\dot{\theta} \leq -1.48) \wedge (\theta > -0.02)$ 2: $(\dot{\theta} > -1.48)$
	1	0: $(\dot{\theta} \leq -0.08) \wedge (\theta \leq -1.45)$ 1: $(\dot{\theta} > -0.08) \wedge (\theta \leq -1.45)$ 2: $(\theta \leq 2.05) \wedge (\theta > -1.45)$ 3: $(\theta \leq 2.50) \wedge (\theta > 2.05)$ 4: $(\dot{\theta} \leq -0.40) \wedge (\theta > 2.50)$ 5: $(\dot{\theta} \leq 0.03) \wedge (\dot{\theta} > -0.40) \wedge (\theta > 2.50)$ 6: $(\dot{\theta} > 0.03) \wedge (\theta > 2.50)$
	2	0: $(\dot{\theta} \leq -0.56)$ 1: $(\dot{\theta} > -0.56) \wedge (\theta \leq -2.16)$ 2: $(\dot{\theta} > -0.56) \wedge (\theta \leq 2.44) \wedge (\theta > -2.16)$ 3: $(\text{conflict}) \wedge (\theta > 2.44)$ 4: $(\dot{\theta} > -0.56) \wedge (\theta > 2.44)$
	3	0: $(\theta \leq -2.18)$ 1: $(\theta \leq 0.04) \wedge (\theta > -2.18)$ 2: $(\theta \leq 2.65) \wedge (\theta > 0.04)$ 3: $(\dot{\theta} \leq -0.21) \wedge (\theta > 2.65)$ 4: $(\dot{\theta} > -0.21) \wedge (\theta > 2.65)$

Table S11: Logic program of CfC in classical control (Pendulum).

Model	Neuron	Logic Program
CfC	0	0: $(\theta \leq -0.03)$ 1: (conflict) 2: (conflict) 3: $(\theta > -0.03)$
	1	0: $(\theta \leq -0.05)$ 1: (conflict) 2: (conflict) 3: $(\theta > -0.05)$
	2	0: $(\theta \leq -2.02)$ 1: $(\theta > -2.02)$
	3	0: $(\theta \leq -0.12)$ 1: $(\theta \leq 0.24) \wedge (\theta > -0.12)$ 2: $(\theta \leq 2.14) \wedge (\theta > 0.24)$ 3: $(\theta > 2.14)$

Table S12: Logic program of NCP in classical control (Pendulum).

Model	Neuron	Logic Program
NCP	0	0: $(\dot{\theta} \leq 0.33)$ 1: $(\dot{\theta} > 0.33)$
	1	0: $(\theta \leq -0.07)$ 1: (conflict) 2: $(\theta \leq 0.27) \wedge (\theta > -0.07)$ 3: $(\theta > 0.27)$
	2	0: $(\dot{\theta} \leq 4.80) \wedge (\theta \leq -1.27)$ 1: $(\dot{\theta} \leq 4.80) \wedge (\theta \leq 1.66) \wedge (\theta > -1.27)$ 2: $(\dot{\theta} \leq 4.80) \wedge (\theta > 1.66)$ 3: $(\dot{\theta} > 4.80)$
	3	0: $(\dot{\theta} \leq -0.33)$ 1: $(\dot{\theta} \leq 0.44) \wedge (\dot{\theta} > -0.33)$ 2: $(\dot{\theta} > 0.44) \wedge (\theta \leq -1.31)$ 3: $(\dot{\theta} > 0.44) \wedge (\theta \leq 1.44) \wedge (\theta > -1.31)$ 4: $(\dot{\theta} > 0.44) \wedge (\theta > 1.44)$

Table S13: Logic program of FC in locomotion (HalfCheetah).

Model	Neuron	Logic Program
FC	0	0: $(\dot{\theta}_R \leq -0.22) \wedge (\dot{\theta}_{T,F} \leq -3.26)$ 1: $(\dot{\theta}_R > -0.22) \wedge (\dot{\theta}_{T,F} \leq -3.26)$ 2: $(\dot{\theta}_{T,F} \leq 6.46) \wedge (\dot{\theta}_{T,F} > -3.26) \wedge (\theta_{F,F} \leq -0.50)$ 3: $(\dot{\theta}_{T,F} \leq 6.46) \wedge (\dot{\theta}_{T,F} > -3.26) \wedge (\theta_{F,F} > -0.50)$ 4: $(\dot{\theta}_{T,F} > 6.46) \wedge (h_R \leq 0.05)$ 5: $(\dot{\theta}_{T,F} > 6.46) \wedge (h_R > 0.05)$
	1	0: $(\theta_{F,B} \leq -0.05) \wedge (\theta_{S,F} \leq 0.61) \wedge (\theta_{T,B} \leq 0.05)$ 1: $(\theta_{F,B} \leq -0.05) \wedge (\theta_{S,F} > 0.61) \wedge (\theta_{T,B} \leq 0.05)$ 2: $(\dot{\theta}_{T,F} \leq -11.24) \wedge (\theta_{F,B} > -0.05) \wedge (\theta_{T,B} \leq 0.05)$ 3: $(\dot{\theta}_{T,F} > -11.24) \wedge (\theta_{F,B} > -0.05) \wedge (\theta_{T,B} \leq 0.05)$ 4: $(\theta_{T,B} > 0.05) \wedge (\theta_{T,F} \leq 0.40)$ 5: $(\theta_{T,B} > 0.05) \wedge (\theta_{T,F} \leq 0.62) \wedge (\theta_{T,F} > 0.40)$ 6: $(\dot{\theta}_{T,B} \leq 2.08) \wedge (\theta_{T,B} > 0.05) \wedge (\theta_{T,F} > 0.62)$ 7: $(\dot{\theta}_{T,B} > 2.08) \wedge (\theta_{T,B} > 0.05) \wedge (\theta_{T,F} > 0.62)$
	2	0: $(\theta_{F,F} \leq -12.45) \wedge (\theta_{F,B} \leq 0.06)$ 1: $(\theta_{F,F} > -12.45) \wedge (\theta_{F,B} \leq 0.06) \wedge (\theta_{S,F} \leq 0.65)$ 2: $(\theta_{F,F} > -12.45) \wedge (\theta_{F,B} \leq 0.06) \wedge (\theta_{S,F} > 0.65)$ 3: $(\dot{\theta}_{T,B} \leq 6.33) \wedge (\theta_{F,B} > 0.06) \wedge (\theta_{T,F} \leq 0.33)$ 4: $(\dot{\theta}_{T,B} \leq 6.33) \wedge (\theta_{F,B} > 0.06) \wedge (\theta_{T,F} > 0.33)$ 5: $(\dot{\theta}_{T,B} > 6.33) \wedge (\theta_{F,B} > 0.06)$
	3	0: $(\theta_{F,B} \leq 0.38) \wedge (\theta_{S,F} \leq 0.17) \wedge (\theta_{T,F} \leq 0.58)$ 1: $(\theta_{F,B} \leq 0.38) \wedge (\theta_{S,F} \leq 0.17) \wedge (\theta_{T,F} > 0.58)$ 2: $(\theta_{F,B} \leq 0.38) \wedge (\theta_{S,F} > 0.17) \wedge (\theta_{T,B} \leq 0.07)$ 3: $(\theta_{F,B} \leq 0.38) \wedge (\theta_{S,F} > 0.17) \wedge (\theta_{T,B} > 0.07)$ 4: $(\theta_{F,B} > 0.38)$
	4	0: $(\theta_{S,B} \leq 1.79) \wedge (\theta_R \leq 0.19) \wedge (\theta_{T,B} \leq 0.06)$ 1: $(\theta_{S,B} > 1.79) \wedge (\theta_R \leq 0.19) \wedge (\theta_{T,B} \leq 0.06)$ 2: $(\dot{\theta}_{F,F} \leq 9.07) \wedge (\theta_R > 0.19) \wedge (\theta_{T,B} \leq 0.06)$ 3: $(\dot{\theta}_{F,F} > 9.07) \wedge (\theta_R > 0.19) \wedge (\theta_{T,B} \leq 0.06)$ 4: $(\theta_R \leq -0.03) \wedge (\theta_{T,B} > 0.06)$ 5: $(\theta_R > -0.03) \wedge (\theta_{F,F} \leq -0.49) \wedge (\theta_{T,B} > 0.06)$ 6: $(\theta_R > -0.03) \wedge (\theta_{F,F} > -0.49) \wedge (\theta_{T,B} > 0.06)$
	5	0: $(\dot{\theta}_{T,B} \leq 1.10) \wedge (\dot{\theta}_{T,F} \leq -6.72) \wedge (\theta_{T,F} \leq 0.67)$ 1: $(\dot{\theta}_{T,B} \leq 1.10) \wedge (\dot{\theta}_{T,F} > -6.72) \wedge (\theta_{T,F} \leq 0.67)$ 2: $(\dot{\theta}_{T,B} \leq 1.10) \wedge (\theta_{T,F} > 0.67)$ 3: $(\dot{\theta}_{T,B} > 1.10) \wedge (h_R \leq -0.33) \wedge (\theta_R \leq 0.29)$ 4: $(\dot{\theta}_{T,B} > 1.10) \wedge (h_R > -0.33) \wedge (\theta_R \leq 0.29)$ 5: $(\dot{\theta}_{T,B} > 1.10) \wedge (h_R \leq -0.48) \wedge (\theta_R > 0.29)$ 6: $(\dot{\theta}_{T,B} > 1.10) \wedge (h_R > -0.48) \wedge (\theta_R > 0.29)$
	6	0: $(\dot{\theta}_R \leq -0.83) \wedge (\dot{\theta}_{F,B} \leq 4.65) \wedge (\dot{\theta}_{F,F} \leq -0.07)$ 1: $(\dot{\theta}_R \leq -0.83) \wedge (\dot{\theta}_{F,B} > 4.65) \wedge (\dot{\theta}_{F,F} \leq -0.07)$ 2: $(\dot{\theta}_R > -0.83) \wedge (\dot{\theta}_{F,F} \leq -0.07) \wedge (\theta_{S,B} \leq -0.33)$ 3: $(\dot{\theta}_R > -0.83) \wedge (\dot{\theta}_{F,F} \leq -0.07) \wedge (\theta_{S,B} > -0.33)$ 4: $(\dot{\theta}_{F,F} > -0.07) \wedge (\theta_R \leq 0.52)$ 5: $(\dot{\theta}_{F,F} > -0.07) \wedge (\theta_R > 0.52)$
	7	0: $(\dot{\theta}_{T,F} \leq -0.36) \wedge (\theta_R \leq 0.33) \wedge (\theta_{S,F} \leq 0.56)$ 1: $(\dot{\theta}_{T,F} \leq -0.36) \wedge (\theta_R > 0.33) \wedge (\theta_{S,F} \leq 0.56)$ 2: $(\dot{\theta}_{T,F} \leq -0.36) \wedge (\theta_{S,F} > 0.56)$ 3: $(\dot{\theta}_{T,F} \leq 6.91) \wedge (\dot{\theta}_{T,F} > -0.36) \wedge (\theta_{S,B} \leq 0.09)$ 4: $(\dot{\theta}_{T,F} > 6.91) \wedge (\theta_{S,B} \leq 0.09)$ 5: $(\dot{\theta}_{T,F} > -0.36) \wedge (\theta_{S,B} > 0.09)$
	8	0: $(\dot{\theta}_R \leq -0.10) \wedge (\dot{\theta}_{T,B} \leq -3.31)$ 1: $(\dot{\theta}_R > -0.10) \wedge (\dot{\theta}_{T,B} \leq -3.31)$ 2: $(\dot{\theta}_{T,B} \leq 0.97) \wedge (\dot{\theta}_{T,B} > -3.31)$ 3: $(\dot{\theta}_{T,B} > 0.97) \wedge (\theta_{S,B} \leq -0.35)$ 4: $(\dot{\theta}_{T,B} > 0.97) \wedge (\theta_R \leq 0.20) \wedge (\theta_{S,B} > -0.35)$ 5: $(\dot{\theta}_{T,B} > 0.97) \wedge (\theta_R > 0.20) \wedge (\theta_{S,B} > -0.35)$
	9	0: $(\dot{\theta}_{F,B} \leq 0.63) \wedge (\dot{\theta}_{S,F} \leq 3.07)$ 1: $(\dot{\theta}_{F,B} \leq 0.63) \wedge (\dot{\theta}_{S,F} > 3.07) \wedge (\theta_R \leq 0.46)$ 2: $(\dot{\theta}_{F,B} \leq 0.63) \wedge (\dot{\theta}_{S,F} > 3.07) \wedge (\theta_R > 0.46)$ 3: $(\dot{\theta}_{F,B} > 0.63) \wedge (\dot{\theta}_{T,F} \leq 5.96) \wedge (h_R \leq 0.03)$ 4: $(\dot{\theta}_{F,B} > 0.63) \wedge (\dot{\theta}_{T,F} \leq 5.96) \wedge (h_R > 0.03)$ 5: $(\dot{\theta}_{F,B} > 0.63) \wedge (\dot{\theta}_{T,F} > 5.96) \wedge (\theta_{T,F} \leq 0.38)$ 6: $(\dot{\theta}_{F,B} > 0.63) \wedge (\dot{\theta}_{T,F} > 5.96) \wedge (\theta_{T,F} > 0.38)$

Table S14: Logic program of GRU in locomotion (HalfCheetah).

Model	Neuron	Logic Program
GRU	0	0: $(\theta_R \leq 1.54) \wedge (\theta_{T,B} \leq -2.33) \wedge (\theta_R \leq 0.52)$ 1: $(\theta_R > 1.54) \wedge (\theta_{T,B} \leq -2.33) \wedge (\theta_R \leq 0.52)$ 2: $(\theta_{T,B} > -2.33) \wedge (\theta_R \leq 0.11)$ 3: $(\theta_{T,B} > -2.33) \wedge (\theta_R \leq 0.52) \wedge (\theta_R > 0.11)$ 4: $(\theta_{T,F} \leq -7.48) \wedge (\theta_R > 0.52)$ 5: $(\theta_{T,F} > -7.48) \wedge (\theta_R \leq 0.97) \wedge (\theta_R > 0.52)$ 6: $(\theta_{T,F} > -7.48) \wedge (\theta_R > 0.97)$
	1	0: $(\theta_{S,B} \leq 10.33) \wedge (\theta_R \leq 0.50) \wedge (\theta_{F,B} \leq -0.41)$ 1: $(\theta_{S,B} \leq 10.33) \wedge (\theta_R \leq 0.50) \wedge (\theta_{F,B} > -0.41)$ 2: $(\theta_{S,B} \leq 10.33) \wedge (h_R \leq -0.07) \wedge (\theta_R > 0.50)$ 3: $(\theta_{S,B} \leq 10.33) \wedge (h_R > -0.07) \wedge (\theta_R > 0.50)$ 4: $(\theta_{S,B} > 10.33)$
	2	0: $(\theta_{T,B} \leq 3.33) \wedge (\theta_R \leq 0.12)$ 1: $(\theta_{T,B} > 3.33) \wedge (\theta_R \leq 0.12)$ 2: $(\theta_{T,B} \leq 6.59) \wedge (\theta_R > 0.12) \wedge (\theta_{T,F} \leq 0.70)$ 3: $(\theta_{T,B} \leq 6.59) \wedge (\theta_R > 0.12) \wedge (\theta_{T,F} > 0.70)$ 4: $(\theta_{T,B} > 6.59) \wedge (\theta_R \leq 0.54) \wedge (\theta_R > 0.12)$ 5: $(\theta_{T,B} > 6.59) \wedge (\theta_R > 0.54)$
	3	0: $(\theta_R \leq -0.78) \wedge (\theta_{T,F} \leq 0.17)$ 1: $(\theta_R > -0.78) \wedge (\theta_R \leq 0.68) \wedge (\theta_{T,F} \leq 0.17)$ 2: $(\theta_R > -0.78) \wedge (\theta_R > 0.68) \wedge (\theta_{T,F} \leq 0.17)$ 3: $(h_R \leq 0.64) \wedge (\theta_{T,B} \leq -0.14) \wedge (\theta_{T,F} > 0.17)$ 4: $(h_R \leq 0.64) \wedge (\theta_{T,B} > -0.14) \wedge (\theta_{T,F} > 0.17)$ 5: $(h_R > 0.64) \wedge (\theta_{T,F} > 0.17)$
	4	0: $(\theta_{S,B} \leq 1.92) \wedge (\theta_{S,F} \leq 0.02)$ 1: $(\theta_{S,B} > 1.92) \wedge (\theta_{S,F} \leq 0.02)$ 2: $(\theta_{S,B} \leq 6.10) \wedge (\theta_{S,F} \leq 7.21) \wedge (\theta_{S,F} > 0.02)$ 3: $(\theta_{S,B} \leq 6.10) \wedge (\theta_{S,F} > 7.21) \wedge (\theta_{S,F} > 0.02)$ 4: $(\theta_{S,B} > 6.10) \wedge (\theta_{S,F} > 0.02)$
	5	0: $(\theta_{T,B} \leq 2.59) \wedge (\theta_{F,B} \leq 0.10) \wedge (\theta_{T,B} \leq -0.16)$ 1: $(\theta_{T,B} \leq 2.59) \wedge (\theta_{F,B} \leq 0.10) \wedge (\theta_{T,B} > -0.16)$ 2: $(\theta_{T,B} > 2.59) \wedge (\theta_{F,B} \leq 0.10)$ 3: $(\theta_{T,B} \leq 1.45) \wedge (\theta_{T,F} \leq 6.43) \wedge (\theta_{F,B} > 0.10)$ 4: $(\theta_{T,B} > 1.45) \wedge (\theta_{T,F} \leq 6.43) \wedge (\theta_{F,B} > 0.10)$ 5: $(\text{conflict}) \wedge (\theta_{F,B} > 0.10)$ 6: $(\theta_{T,F} > 6.43) \wedge (\theta_{F,B} > 0.10)$
	6	0: $(\theta_R \leq 0.17) \wedge (\theta_{F,B} \leq -0.12)$ 1: $(\theta_R \leq 0.62) \wedge (\theta_R > 0.17) \wedge (\theta_{F,B} \leq -0.12)$ 2: $(\theta_{F,B} \leq 6.66) \wedge (\theta_R \leq 0.62) \wedge (\theta_{F,B} > -0.12)$ 3: $(\theta_{F,B} > 6.66) \wedge (\theta_R \leq 0.62) \wedge (\theta_{F,B} > -0.12)$ 4: $(\theta_{T,B} \leq -5.47) \wedge (\theta_R > 0.62)$ 5: $(\theta_{T,B} > -5.47) \wedge (\theta_R \leq 0.89) \wedge (\theta_R > 0.62)$ 6: $(\theta_{T,B} > -5.47) \wedge (\theta_R > 0.89)$
	7	0: $(h_R \leq -0.27) \wedge (\theta_{T,F} \leq 0.20)$ 1: $(\theta_{T,B} \leq -0.25) \wedge (h_R > -0.27) \wedge (\theta_{T,F} \leq 0.20)$ 2: $(\theta_{T,B} > -0.25) \wedge (h_R > -0.27) \wedge (\theta_{T,F} \leq 0.20)$ 3: $(h_R \leq 0.12) \wedge (\theta_R \leq 0.77) \wedge (\theta_{T,F} > 0.20)$ 4: $(h_R \leq 0.12) \wedge (\theta_R > 0.77) \wedge (\theta_{T,F} > 0.20)$ 5: $(h_R > 0.12) \wedge (\theta_{T,F} > 0.20)$
	8	0: $(h_R \leq 0.13) \wedge (\theta_{F,B} \leq -0.16) \wedge (h_R \leq 0.07)$ 1: $(h_R \leq 0.13) \wedge (\theta_{F,B} > -0.16) \wedge (h_R \leq 0.07)$ 2: $(h_R \leq 0.13) \wedge (h_R > 0.07)$ 3: $(h_R \leq 1.11) \wedge (h_R > 0.13) \wedge (h_R \leq 0.08)$ 4: $(h_R > 1.11) \wedge (h_R \leq 0.08)$ 5: $(h_R > 0.13) \wedge (h_R > 0.08)$
	9	0: $(\theta_{T,F} \leq 0.51) \wedge (\theta_{S,F} \leq -0.07)$ 1: $(\theta_{F,F} \leq 3.81) \wedge (\theta_{T,F} \leq 0.51) \wedge (\theta_{S,F} > -0.07)$ 2: $(\theta_{F,F} > 3.81) \wedge (\theta_{T,F} \leq 0.51) \wedge (\theta_{S,F} > -0.07)$ 3: $(\theta_{T,F} > 0.51) \wedge (\theta_{F,B} \leq 0.34)$ 4: $(\theta_R \leq -1.78) \wedge (\theta_{T,F} > 0.51) \wedge (\theta_{F,B} > 0.34)$ 5: $(\theta_R > -1.78) \wedge (\theta_{T,F} > 0.51) \wedge (\theta_{F,B} > 0.34)$

Table S15: Logic program of LSTM in locomotion (HalfCheetah).

Model	Neuron	Logic Program
LSTM	0	0: $(\dot{\theta}_R \leq 2.01) \wedge (\theta_{S,B} \leq 0.53) \wedge (\theta_{T,F} \leq -0.28)$ 1: $(\dot{\theta}_R \leq 2.01) \wedge (\theta_{S,B} \leq 0.53) \wedge (\theta_{T,F} > -0.28)$ 2: $(\dot{\theta}_R > 2.01) \wedge (\theta_{S,B} \leq 0.53)$ 3: $(\theta_{S,B} > 0.53)$
	1	0: $(\theta_{F,F} \leq 0.02) \wedge (\theta_{T,F} \leq -0.35)$ 1: $(\dot{\theta}_{F,F} \leq 1.23) \wedge (\theta_{F,F} \leq 0.02) \wedge (\theta_{T,F} > -0.35)$ 2: $(\dot{\theta}_{F,F} > 1.23) \wedge (\theta_{F,F} \leq 0.02) \wedge (\theta_{T,F} > -0.35)$ 3: $(\theta_{F,F} > 0.02) \wedge (\theta_{T,F} \leq -0.07)$ 4: $(\dot{\theta}_{F,F} \leq 0.95) \wedge (\theta_{F,F} > 0.02) \wedge (\theta_{T,F} > -0.07)$ 5: $(\dot{\theta}_{F,F} > 0.95) \wedge (\theta_{F,F} > 0.02) \wedge (\theta_{T,F} > -0.07)$
	2	0: $(\theta_{F,F} \leq -0.46) \wedge (h_R \leq -0.07)$ 1: $(\dot{\theta}_{F,B} \leq -4.76) \wedge (\theta_{F,F} > -0.46) \wedge (h_R \leq -0.07)$ 2: $(\dot{\theta}_{F,B} > -4.76) \wedge (\theta_{F,F} > -0.46) \wedge (h_R \leq -0.07)$ 3: $(\theta_R \leq 0.11) \wedge (h_R > -0.07)$ 4: $(\theta_R > 0.11) \wedge (h_R > -0.07)$
	3	0: $(\dot{\theta}_{S,B} \leq 0.14) \wedge (\theta_{T,F} \leq -0.01) \wedge (h_R \leq -0.11)$ 1: $(\dot{\theta}_{S,B} \leq 0.14) \wedge (\theta_{T,F} > -0.01) \wedge (h_R \leq -0.11)$ 2: $(\dot{\theta}_{S,B} > 0.14) \wedge (\theta_{S,B} \leq 0.42) \wedge (h_R \leq -0.11)$ 3: $(\dot{\theta}_{S,B} > 0.14) \wedge (\theta_{S,B} > 0.42) \wedge (h_R \leq -0.11)$ 4: $(\theta_{T,B} \leq 0.27) \wedge (h_R > -0.11)$ 5: $(\theta_{T,B} \leq 0.53) \wedge (\theta_{T,B} > 0.27) \wedge (h_R > -0.11)$ 6: $(\theta_{T,B} > 0.53) \wedge (h_R > -0.11)$
	4	0: $(\theta_{F,F} \leq -0.00)$ 1: (conflict) 2: $(\theta_R \leq 0.12) \wedge (\theta_{F,F} \leq 0.39) \wedge (\theta_{F,F} > -0.00)$ 3: $(\theta_R > 0.12) \wedge (\theta_{F,F} \leq 0.39) \wedge (\theta_{F,F} > -0.00)$ 4: $(\dot{\theta}_R \leq -0.51) \wedge (\theta_{F,F} > 0.39)$ 5: $(\dot{\theta}_R > -0.51) \wedge (\theta_{F,F} > 0.39)$
	5	0: $(\dot{\theta}_R \leq 0.07) \wedge (\theta_{F,F} \leq -0.05)$ 1: $(\dot{\theta}_R \leq 0.07) \wedge (\theta_{F,F} \leq 0.35) \wedge (\theta_{F,F} > -0.05)$ 2: $(\dot{\theta}_R > 0.07) \wedge (\theta_{F,F} \leq 0.35) \wedge (h_R \leq -0.18)$ 3: $(\dot{\theta}_R > 0.07) \wedge (\theta_{F,F} \leq 0.35) \wedge (h_R > -0.18)$ 4: $(\dot{\theta}_{S,B} \leq -2.15) \wedge (\theta_{F,F} > 0.35)$ 5: $(\dot{\theta}_{S,B} > -2.15) \wedge (\theta_{F,F} > 0.35)$
	6	0: $(\dot{\theta}_{T,F} \leq 1.81) \wedge (h_R \leq -1.08) \wedge (\theta_{T,F} \leq -0.14)$ 1: $(\dot{\theta}_{T,F} \leq 1.81) \wedge (h_R > -1.08) \wedge (\theta_{T,F} \leq -0.14)$ 2: $(\dot{\theta}_{T,F} > 1.81) \wedge (\theta_{T,F} \leq -0.14)$ 3: $(h_R \leq -0.47) \wedge (\theta_{T,F} > -0.14)$ 4: $(\dot{\theta}_{T,B} \leq -1.89) \wedge (h_R > -0.47) \wedge (\theta_{T,F} > -0.14)$ 5: $(\dot{\theta}_{T,B} > -1.89) \wedge (h_R > -0.47) \wedge (\theta_{T,F} > -0.14)$
	7	0: $(\theta_{F,F} \leq -0.07) \wedge (\theta_{T,F} \leq 0.36)$ 1: $(\theta_{F,F} \leq -0.07) \wedge (\theta_{T,F} > 0.36)$ 2: $(\dot{x}_R \leq 4.14) \wedge (\theta_{F,F} > -0.07) \wedge (\theta_{T,B} \leq 0.34)$ 3: $(\dot{x}_R > 4.14) \wedge (\theta_{F,F} > -0.07) \wedge (\theta_{T,B} \leq 0.34)$ 4: $(\dot{\theta}_{T,F} \leq -2.37) \wedge (\theta_{F,F} > -0.07) \wedge (\theta_{T,B} > 0.34)$ 5: $(\dot{\theta}_{T,F} > -2.37) \wedge (\theta_{F,F} > -0.07) \wedge (\theta_{T,B} > 0.34)$
	8	0: $(\dot{\theta}_{F,B} \leq 11.09) \wedge (\dot{\theta}_{F,F} \leq 1.05) \wedge (\theta_{T,F} \leq -0.46)$ 1: $(\dot{\theta}_{F,B} \leq 11.09) \wedge (\dot{\theta}_{F,F} \leq 1.05) \wedge (\theta_{T,F} > -0.46)$ 2: $(\dot{\theta}_{F,B} > 11.09) \wedge (\dot{\theta}_{F,F} \leq 1.05)$ 3: $(\dot{\theta}_{F,F} > 1.05) \wedge (\dot{\theta}_{T,B} \leq -11.38)$ 4: $(\dot{\theta}_{F,F} > 1.05) \wedge (\dot{\theta}_{T,B} > -11.38) \wedge (\theta_R \leq 0.16)$ 5: $(\dot{\theta}_{F,F} > 1.05) \wedge (\dot{\theta}_{T,B} > -11.38) \wedge (\theta_R > 0.16)$
	9	0: $(\theta_{F,F} \leq -0.40) \wedge (\theta_{S,B} \leq -0.33)$ 1: $(\theta_{F,F} \leq -0.40) \wedge (\theta_{S,B} > -0.33)$ 2: $(\dot{\theta}_{T,F} \leq -10.21) \wedge (h_R \leq -0.80) \wedge (\theta_{F,F} > -0.40)$ 3: $(\dot{\theta}_{T,F} > -10.21) \wedge (h_R \leq -0.80) \wedge (\theta_{F,F} > -0.40)$ 4: $(h_R > -0.80) \wedge (\theta_{F,B} \leq -0.14) \wedge (\theta_{F,F} > -0.40)$ 5: $(h_R > -0.80) \wedge (\theta_{F,B} > -0.14) \wedge (\theta_{F,F} > -0.40)$

Table S16: Logic program of ODE-RNN in locomotion (HalfCheetah).

Model	Neuron	Logic Program
ODE-RNN	0	0: ($\dot{h}_R \leq -0.27$) \wedge ($\theta_{S,B} \leq -0.49$) 1: ($\dot{h}_R > -0.27$) \wedge ($\theta_{S,B} \leq -0.49$) 2: ($\dot{h}_R \leq -0.00$) \wedge ($\theta_{F,F} \leq -0.22$) \wedge ($\theta_{S,B} > -0.49$) 3: ($\dot{h}_R \leq -0.00$) \wedge ($\theta_{F,F} > -0.22$) \wedge ($\theta_{S,B} > -0.49$) 4: ($\dot{h}_R > -0.00$) \wedge ($\theta_{S,B} > -0.49$) \wedge ($\theta_{T,B} \leq 0.22$) 5: ($\dot{h}_R > -0.00$) \wedge ($\theta_{S,B} > -0.49$) \wedge ($\theta_{T,B} > 0.22$)
	1	0: ($\dot{\theta}_{T,B} \leq -2.91$) \wedge ($\theta_{F,B} \leq -0.39$) 1: ($\dot{\theta}_{T,B} > -2.91$) \wedge ($\dot{h}_R \leq -0.21$) \wedge ($\theta_{F,B} \leq -0.39$) 2: ($\dot{\theta}_{T,B} > -2.91$) \wedge ($\dot{h}_R > -0.21$) \wedge ($\theta_{F,B} \leq -0.39$) 3: ($\dot{\theta}_{T,B} \leq -0.00$) \wedge ($\theta_{F,B} > -0.39$) 4: ($\dot{\theta}_R > -0.00$) \wedge ($\theta_R \leq -0.04$) \wedge ($\theta_{F,B} > -0.39$) 5: ($\dot{\theta}_R > -0.00$) \wedge ($\theta_R > -0.04$) \wedge ($\theta_{F,B} > -0.39$)
	2	0: ($\theta_R \leq 0.02$) \wedge ($\theta_{T,B} \leq -0.16$) 1: ($\theta_R \leq 0.02$) \wedge ($\theta_{T,B} > -0.16$) \wedge ($h_R \leq 0.00$) 2: ($\theta_R \leq 0.02$) \wedge ($\theta_{T,B} > -0.16$) \wedge ($h_R > 0.00$) 3: ($\theta_R > 0.02$) \wedge ($h_R \leq -0.02$) 4: ($\theta_R > 0.02$) \wedge (conflict) 5: ($\theta_R > 0.02$) \wedge ($h_R > -0.02$)
	3	0: ($\dot{h}_R \leq 0.55$) \wedge ($\theta_R \leq 0.08$) \wedge ($\theta_{T,B} \leq 0.42$) 1: ($\dot{h}_R > 0.55$) \wedge ($\theta_R \leq 0.08$) \wedge ($\theta_{T,B} \leq 0.42$) 2: ($\theta_R \leq 0.08$) \wedge ($\theta_{S,B} \leq 0.16$) \wedge ($\theta_{T,B} > 0.42$) 3: ($\theta_R \leq 0.08$) \wedge ($\theta_{S,B} > 0.16$) \wedge ($\theta_{T,B} > 0.42$) 4: ($\theta_R > 0.08$) \wedge ($\theta_{T,B} \leq 0.42$) \wedge ($h_R \leq -0.05$) 5: ($\theta_R > 0.08$) \wedge ($\theta_{T,B} \leq 0.42$) \wedge ($h_R > -0.05$) 6: ($\theta_R > 0.08$) \wedge ($\theta_{T,B} > 0.42$)
	4	0: ($\dot{\theta}_{T,B} \leq -3.83$) \wedge ($\dot{\theta}_{T,F} \leq -0.87$) 1: ($\dot{\theta}_{T,B} \leq -3.83$) \wedge ($\dot{\theta}_{T,F} > -0.87$) \wedge ($h_R \leq -0.08$) 2: ($\dot{\theta}_{T,B} \leq -3.83$) \wedge ($\dot{\theta}_{T,F} > -0.87$) \wedge ($h_R > -0.08$) 3: ($\dot{\theta}_{T,B} > -3.83$) \wedge ($\theta_{S,B} \leq -0.11$) \wedge ($h_R \leq -0.09$) 4: ($\dot{\theta}_{T,B} > -3.83$) \wedge ($\theta_{S,B} > -0.11$) \wedge ($h_R \leq -0.09$) 5: ($\dot{\theta}_{T,B} > -3.83$) \wedge ($\theta_{T,B} \leq -0.33$) \wedge ($h_R > -0.09$) 6: ($\dot{\theta}_{T,B} > -3.83$) \wedge ($\theta_{T,B} > -0.33$) \wedge ($h_R > -0.09$)
	5	0: ($\dot{x}_R \leq 3.31$) 1: ($\dot{x}_R > 3.31$) \wedge ($\theta_{S,B} \leq 0.01$) \wedge ($\theta_{T,F} \leq 0.57$) 2: ($\dot{x}_R > 3.31$) \wedge ($\theta_{S,B} > 0.01$) \wedge ($\theta_{T,F} \leq 0.57$) 3: ($\dot{x}_R > 3.31$) \wedge ($\theta_{T,F} > 0.57$)
	6	0: ($\dot{\theta}_{T,B} \leq 1.22$) \wedge ($\theta_{S,B} \leq -0.54$) 1: ($\dot{\theta}_{T,B} > 1.22$) \wedge ($\theta_{S,B} \leq -0.54$) 2: ($\dot{\theta}_{T,B} \leq -3.70$) \wedge ($\theta_{S,B} > -0.54$) \wedge ($\theta_{T,B} \leq 0.16$) 3: ($\dot{\theta}_{T,B} \leq -3.70$) \wedge ($\theta_{S,B} > -0.54$) \wedge ($\theta_{T,B} > 0.16$) 4: ($\dot{\theta}_{T,B} > -3.70$) \wedge (conflict) 5: ($\dot{\theta}_{T,B} > -3.70$) \wedge ($\theta_{S,B} > -0.54$)
	7	0: ($\dot{h}_R \leq 0.02$) \wedge ($\theta_{S,F} \leq -0.19$) \wedge ($\theta_{T,B} \leq 0.53$) 1: ($\dot{h}_R \leq 0.02$) \wedge ($\theta_{S,F} \leq -0.19$) \wedge ($\theta_{T,B} > 0.53$) 2: ($\dot{h}_R > 0.02$) \wedge ($\theta_{S,F} \leq -0.19$) 3: ($\dot{\theta}_R \leq 0.53$) \wedge ($\theta_{S,F} \leq 0.16$) \wedge ($\theta_{S,F} > -0.19$) 4: ($\dot{\theta}_R \leq 0.53$) \wedge ($\theta_{S,F} > 0.16$) 5: ($\dot{\theta}_R > 0.53$) \wedge ($\theta_{S,F} > -0.19$)
	8	0: ($\dot{\theta}_{T,B} \leq -0.39$) \wedge ($\theta_{T,B} \leq -0.37$) 1: ($\dot{\theta}_{T,B} \leq -0.39$) \wedge ($\theta_{S,B} \leq 0.04$) \wedge ($\theta_{T,B} > -0.37$) 2: ($\dot{\theta}_{T,B} \leq -0.39$) \wedge ($\theta_{S,B} > 0.04$) \wedge ($\theta_{T,B} > -0.37$) 3: ($\dot{\theta}_{T,B} > -0.39$) \wedge ($\theta_{T,B} \leq 0.55$) \wedge ($\theta_{T,F} \leq 0.09$) 4: ($\dot{\theta}_{T,B} > -0.39$) \wedge ($\theta_{T,B} \leq 0.55$) \wedge ($\theta_{T,F} > 0.09$) 5: ($\dot{\theta}_{T,B} > -0.39$) \wedge ($\theta_{T,B} > 0.55$)
	9	0: ($\theta_{T,F} \leq -0.24$) 1: ($\dot{\theta}_{T,F} \leq -6.60$) \wedge (conflict) 2: ($\dot{\theta}_{T,F} > -6.60$) \wedge (conflict) 3: ($\theta_{T,F} > -0.24$) \wedge ($h_R \leq -0.11$) 4: ($\theta_{T,F} \leq 0.32$) \wedge ($\theta_{T,F} > -0.24$) \wedge ($h_R > -0.11$) 5: ($\theta_{T,F} > 0.32$) \wedge ($h_R > -0.11$)

Table S17: Logic program of CfC in locomotion (HalfCheetah).

Model	Neuron	Logic Program
CfC	0	0: $(\dot{\theta}_{F,F} \leq -9.40)$ 1: $(\dot{\theta}_{F,F} > -9.40) \wedge (\dot{\theta}_{T,B} \leq -1.68) \wedge (\theta_{F,F} \leq 0.23)$ 2: $(\dot{\theta}_{F,F} > -9.40) \wedge (\dot{\theta}_{T,B} > -1.68) \wedge (\theta_{F,F} \leq 0.23)$ 3: $(\dot{\theta}_{F,F} > -9.40) \wedge (\dot{\theta}_{T,F} \leq -5.69) \wedge (\theta_{F,F} > 0.23)$ 4: $(\dot{\theta}_{F,F} > -9.40) \wedge (\dot{\theta}_{T,F} > -5.69) \wedge (\theta_{F,F} > 0.23)$
	1	0: $(\theta_R \leq 0.06) \wedge (\theta_{T,F} \leq -0.46)$ 1: $(\theta_R > 0.06) \wedge (\theta_{T,F} \leq -0.46)$ 2: $(\theta_R \leq 0.02) \wedge (\theta_{T,F} > -0.46)$ 3: $(\theta_R > 0.02) \wedge (\text{conflict})$ 4: $(\theta_R > 0.02) \wedge (\theta_{T,F} > -0.46)$
	2	0: $(\dot{\theta}_{T,B} \leq 1.92) \wedge (\dot{\theta}_{T,F} \leq -0.59) \wedge (\dot{h}_R \leq 0.43)$ 1: $(\dot{\theta}_{T,B} \leq 1.92) \wedge (\dot{\theta}_{T,F} > -0.59) \wedge (\dot{h}_R \leq 0.43)$ 2: $(\dot{\theta}_{T,B} > 1.92) \wedge (\dot{\theta}_{T,F} \leq 5.02) \wedge (\dot{h}_R \leq 0.43)$ 3: $(\dot{\theta}_{T,B} > 1.92) \wedge (\dot{\theta}_{T,F} > 5.02) \wedge (\dot{h}_R \leq 0.43)$ 4: $(\dot{\theta}_{S,F} \leq 13.53) \wedge (\dot{h}_R > 0.43) \wedge (\theta_{F,B} \leq -0.01)$ 5: $(\dot{\theta}_{S,F} \leq 13.53) \wedge (\dot{h}_R > 0.43) \wedge (\theta_{F,B} > -0.01)$ 6: $(\dot{\theta}_{S,F} > 13.53) \wedge (\dot{h}_R > 0.43)$
	3	0: $(\dot{\theta}_{T,F} \leq 8.70) \wedge (\theta_{S,F} \leq 0.53) \wedge (h_R \leq -0.09)$ 1: $(\dot{\theta}_{T,F} \leq 8.70) \wedge (\theta_{S,F} \leq 0.53) \wedge (h_R > -0.09)$ 2: $(\dot{\theta}_{T,F} \leq 8.70) \wedge (\theta_{S,F} > 0.53)$ 3: $(\dot{\theta}_{T,F} > 8.70) \wedge (\theta_R \leq 0.20)$ 4: $(\dot{\theta}_{T,F} > 8.70) \wedge (\theta_R > 0.20)$
	4	0: $(\theta_{T,F} \leq -0.51) \wedge (h_R \leq -0.04)$ 1: $(\theta_{T,F} \leq -0.51) \wedge (h_R > -0.04)$ 2: $(\dot{\theta}_{T,B} \leq 0.58) \wedge (\theta_{T,F} \leq 0.50) \wedge (\theta_{T,F} > -0.51)$ 3: $(\dot{\theta}_{T,B} \leq 0.58) \wedge (\theta_{T,F} > 0.50)$ 4: $(\dot{\theta}_{T,B} > 0.58) \wedge (\dot{h}_R \leq -0.44) \wedge (\theta_{T,F} > -0.51)$ 5: $(\dot{\theta}_{T,B} > 0.58) \wedge (\dot{h}_R > -0.44) \wedge (\theta_{T,F} > -0.51)$
	5	0: $(\dot{\theta}_{T,B} \leq 2.61) \wedge (\theta_{S,F} \leq 0.08) \wedge (h_R \leq 0.03)$ 1: $(\dot{\theta}_{T,B} \leq 2.61) \wedge (\theta_{S,F} \leq 0.08) \wedge (h_R > 0.03)$ 2: $(\dot{\theta}_R \leq 0.63) \wedge (\dot{\theta}_{T,B} \leq 2.61) \wedge (\theta_{S,F} > 0.08)$ 3: $(\dot{\theta}_R > 0.63) \wedge (\dot{\theta}_{T,B} \leq 2.61) \wedge (\theta_{S,F} > 0.08)$ 4: $(\dot{\theta}_{T,B} > 2.61) \wedge (\theta_{T,F} \leq -0.13)$ 5: $(\dot{\theta}_{T,B} > 2.61) \wedge (\theta_{T,F} > -0.13)$
	6	0: $(\dot{\theta}_{T,B} \leq -0.60) \wedge (\theta_{F,F} \leq -0.11)$ 1: $(\dot{\theta}_{T,B} > -0.60) \wedge (\theta_{F,F} \leq -0.11) \wedge (h_R \leq -0.09)$ 2: $(\dot{\theta}_{T,B} > -0.60) \wedge (\theta_{F,F} \leq -0.11) \wedge (h_R > -0.09)$ 3: $(\dot{\theta}_{S,F} \leq 11.48) \wedge (\theta_{F,F} > -0.11) \wedge (\theta_{T,B} \leq -0.10)$ 4: $(\dot{\theta}_{S,F} \leq 11.48) \wedge (\theta_{F,F} > -0.11) \wedge (\theta_{T,B} > -0.10)$ 5: $(\dot{\theta}_{S,F} > 11.48) \wedge (\theta_{F,F} > -0.11)$
	7	0: $(\dot{\theta}_{T,F} \leq -8.38) \wedge (\dot{h}_R \leq 0.45) \wedge (\theta_{T,F} \leq 0.47)$ 1: $(\dot{\theta}_{T,F} > -8.38) \wedge (\dot{h}_R \leq 0.45) \wedge (\theta_{T,F} \leq 0.47)$ 2: $(\dot{h}_R > 0.45) \wedge (\theta_{F,F} \leq 0.14) \wedge (\theta_{T,F} \leq 0.47)$ 3: $(\dot{h}_R > 0.45) \wedge (\theta_{F,F} > 0.14) \wedge (\theta_{T,F} \leq 0.47)$ 4: $(\theta_{T,F} \leq 0.69) \wedge (\theta_{T,F} > 0.47)$ 5: $(\theta_{T,F} > 0.69)$
	8	0: $(\dot{\theta}_{T,B} \leq -6.34) \wedge (h_R \leq -0.02)$ 1: $(\dot{\theta}_{T,B} > -6.34) \wedge (h_R \leq -0.02)$ 2: $(\dot{\theta}_{T,B} > -6.34) \wedge (\text{conflict})$ 3: $(\dot{\theta}_{T,F} \leq 10.03) \wedge (\theta_{S,F} \leq 0.50) \wedge (h_R > -0.02)$ 4: $(\dot{\theta}_{T,F} > 10.03) \wedge (\theta_{S,F} \leq 0.50) \wedge (h_R > -0.02)$ 5: $(\theta_{S,F} > 0.50) \wedge (h_R > -0.02)$
	9	0: $(\dot{\theta}_{T,B} \leq 1.14) \wedge (\theta_{S,B} \leq -0.06) \wedge (\theta_{S,F} \leq 0.46)$ 1: $(\dot{\theta}_{T,B} \leq 1.14) \wedge (\theta_{S,B} > -0.06) \wedge (\theta_{S,F} \leq 0.46)$ 2: $(\dot{\theta}_{T,B} \leq 1.14) \wedge (\theta_{S,F} > 0.46)$ 3: $(\dot{\theta}_{T,B} > 1.14) \wedge (\theta_{T,F} \leq 0.56) \wedge (h_R \leq -0.10)$ 4: $(\dot{\theta}_{T,B} > 1.14) \wedge (\theta_{T,F} \leq 0.56) \wedge (h_R > -0.10)$ 5: $(\dot{\theta}_{T,B} > 1.14) \wedge (\theta_{T,F} > 0.56)$

Table S18: Logic program of NCP in locomotion (HalfCheetah).

Model	Neuron	Logic Program
NCP	0	0: $(\theta_{F,B} \leq -0.05)$ 1: $(\theta_{F,B} > -0.05)$
	1	0: $(\theta_{F,B} \leq -0.04)$ 1: $(\theta_{F,B} > -0.04)$
	2	0: $(\theta_{T,B} \leq -0.29)$ 1: $(\theta_{T,B} > -0.29)$
	3	0: $(\dot{\theta}_{T,F} \leq -6.91) \wedge (h_R \leq -0.08)$ 1: $(\dot{\theta}_{T,F} \leq -6.91) \wedge (h_R > -0.08)$ 2: $(\dot{\theta}_{T,F} > -6.91) \wedge (\theta_{F,F} \leq -0.13)$ 3: $(\dot{\theta}_{T,F} > -6.91) \wedge (\theta_{F,F} > -0.13)$
	4	0: $(\dot{\theta}_{F,B} \leq -6.37) \wedge (\theta_{T,B} \leq -0.36)$ 1: $(\dot{\theta}_{F,B} > -6.37) \wedge (\theta_{T,B} \leq -0.36)$ 2: $(\dot{h}_R \leq -0.59) \wedge (\theta_{T,B} \leq 0.59) \wedge (\theta_{T,B} > -0.36)$ 3: $(\dot{h}_R > -0.59) \wedge (\theta_{T,B} \leq 0.59) \wedge (\theta_{T,B} > -0.36)$ 4: $(\dot{\theta}_{F,B} \leq 0.64) \wedge (\theta_{T,B} > 0.59)$ 5: $(\dot{\theta}_{F,B} > 0.64) \wedge (\theta_{T,B} > 0.59)$
	5	0: $(\theta_{F,B} \leq -0.02) \wedge (\theta_{T,B} \leq -0.40)$ 1: $(\theta_{F,B} \leq -0.02) \wedge (\theta_{T,B} > -0.40)$ 2: $(\theta_{F,B} > -0.02)$
	6	0: $(\dot{\theta}_{F,F} \leq -3.61) \wedge (\theta_{F,B} \leq -0.06)$ 1: $(\dot{\theta}_{F,F} > -3.61) \wedge (\theta_{F,B} \leq -0.06)$ 2: $(\dot{h}_R \leq 0.51) \wedge (\theta_{F,B} > -0.06) \wedge (\theta_{T,F} \leq -0.70)$ 3: $(\dot{h}_R \leq 0.51) \wedge (\theta_{F,B} > -0.06) \wedge (\theta_{T,F} > -0.70)$ 4: $(\dot{h}_R > 0.51) \wedge (\theta_{F,B} > -0.06)$
	7	0: $(\theta_{T,B} \leq -0.27)$ 1: (conflict) 2: $(\dot{\theta}_{S,F} \leq -8.45) \wedge (\dot{h}_R \leq 0.18) \wedge (\theta_{T,B} > -0.27)$ 3: $(\dot{\theta}_{S,F} \leq -8.45) \wedge (\dot{h}_R > 0.18) \wedge (\theta_{T,B} > -0.27)$ 4: $(\dot{\theta}_{S,F} > -8.45) \wedge (\theta_{F,B} \leq 0.22) \wedge (\theta_{T,B} > -0.27)$ 5: $(\dot{\theta}_{S,F} > -8.45) \wedge (\theta_{F,B} > 0.22) \wedge (\theta_{T,B} > -0.27)$
	8	0: $(\dot{\theta}_{F,B} \leq 6.33) \wedge (\dot{\theta}_{T,F} \leq 12.79) \wedge (\theta_{S,B} \leq -0.04)$ 1: $(\dot{\theta}_{F,B} > 6.33) \wedge (\dot{\theta}_{T,F} \leq 12.79) \wedge (\theta_{S,B} \leq -0.04)$ 2: $(\dot{\theta}_{T,F} \leq 12.79) \wedge (\theta_{S,B} > -0.04)$ 3: $(\dot{\theta}_{T,F} > 12.79)$
9	0: $(\dot{\theta}_{F,B} \leq 6.97) \wedge (h_R \leq -0.12)$ 1: $(\dot{\theta}_{F,B} \leq 6.97) \wedge (\theta_{F,F} \leq 0.15) \wedge (h_R > -0.12)$ 2: $(\dot{\theta}_{F,B} \leq 6.97) \wedge (\theta_{F,F} > 0.15) \wedge (h_R > -0.12)$ 3: $(\dot{\theta}_{F,B} > 6.97) \wedge (\dot{\theta}_{S,B} \leq -8.53)$ 4: $(\dot{\theta}_{F,B} > 6.97) \wedge (\dot{\theta}_{S,B} > -8.53)$	

Table S19: Logic program of FC in end-to-end visual servoing (Image-based Driving).

Model	Neuron	Logic Program
FC	0	0: $(\kappa \leq 0.00) \wedge (v \leq 7.40)$ 1: $(\kappa \leq 0.00) \wedge (v \leq 7.71) \wedge (v > 7.40)$ 2: $(\kappa > 0.00) \wedge (v \leq 7.71)$ 3: $(\kappa \leq 0.00) \wedge (d \leq 0.12) \wedge (v > 7.71)$ 4: $(\kappa \leq 0.00) \wedge (d > 0.12) \wedge (v > 7.71)$ 5: $(\kappa > 0.00) \wedge (v > 7.71)$
	1	0: $(v \leq 7.30)$ 1: $(\delta \leq 0.00) \wedge (d \leq 0.19) \wedge (v > 7.30)$ 2: $(\delta \leq 0.00) \wedge (d > 0.19) \wedge (v > 7.30)$ 3: $(\delta > 0.00) \wedge (d \leq 0.29) \wedge (v > 7.30)$ 4: $(\delta > 0.00) \wedge (d > 0.29) \wedge (v > 7.30)$
	2	0: $(\delta \leq -0.02) \wedge (\kappa \leq 0.02) \wedge (\mu \leq 0.01)$ 1: $(\delta > -0.02) \wedge (\kappa \leq 0.02) \wedge (\mu \leq 0.01)$ 2: $(\kappa > 0.02) \wedge (\mu \leq 0.01)$ 3: $(\mu > 0.01)$
	3	0: $(\kappa \leq -0.00)$ 1: $(\kappa > -0.00) \wedge (\mu \leq 0.01) \wedge (d \leq 0.07)$ 2: $(\kappa > -0.00) \wedge (\mu \leq 0.01) \wedge (d > 0.07)$ 3: $(\kappa > -0.00) \wedge (\mu \leq 0.02) \wedge (\mu > 0.01)$ 4: $(\kappa > -0.00) \wedge (\mu > 0.02)$
	4	0: $(\kappa \leq 0.00) \wedge (\mu \leq 0.01) \wedge (v \leq 7.66)$ 1: $(\kappa \leq 0.00) \wedge (\mu \leq 0.01) \wedge (v > 7.66)$ 2: $(\kappa \leq 0.00) \wedge (\mu > 0.01)$ 3: $(\kappa > 0.00) \wedge (\mu \leq -0.02)$ 4: $(\kappa > 0.00) \wedge (\mu \leq 0.01) \wedge (\mu > -0.02)$ 5: $(\kappa > 0.00) \wedge (\mu > 0.01)$
	5	0: $(\mu \leq 0.01) \wedge (v \leq 7.49)$ 1: $(\delta \leq -0.02) \wedge (\mu \leq 0.01) \wedge (v > 7.49)$ 2: $(\delta > -0.02) \wedge (\mu \leq 0.01) \wedge (v > 7.49)$ 3: $(\mu \leq 0.02) \wedge (\mu > 0.01)$ 4: $(\mu > 0.02)$
	6	0: $(\kappa \leq -0.01)$ 1: $(\delta \leq -0.01) \wedge (\kappa > -0.01) \wedge (\mu \leq 0.01)$ 2: $(\delta > -0.01) \wedge (\kappa > -0.01) \wedge (\mu \leq 0.01)$ 3: $(\kappa > -0.01) \wedge (\mu > 0.01)$
	7	0: $(\mu \leq -0.02)$ 1: $(\delta \leq 0.02) \wedge (\mu \leq 0.01) \wedge (\mu > -0.02)$ 2: $(\delta > 0.02) \wedge (\mu \leq 0.01) \wedge (\mu > -0.02)$ 3: $(\mu > 0.01)$

Table S20: Logic program of GRU in end-to-end visual servoing (Image-based Driving).

Model	Neuron	Logic Program
GRU	0	0: ($d \leq -0.06$) 1: ($d \leq 0.11$) \wedge ($d > -0.06$) 2: ($d > 0.11$)
	1	0: ($\mu \leq 0.04$) 1: ($\mu \leq 0.09$) \wedge ($\mu > 0.04$) 2: ($\mu > 0.09$)
	2	0: ($\mu \leq 0.04$) 1: ($\mu \leq 0.10$) \wedge ($\mu > 0.04$) 2: ($\mu > 0.10$)
	3	0: ($v \leq 5.26$) 1: ($\mu \leq 0.01$) \wedge ($v \leq 6.88$) \wedge ($v > 5.26$) 2: ($\mu > 0.01$) \wedge ($v \leq 6.88$) \wedge ($v > 5.26$) 3: ($v \leq 7.34$) \wedge ($v > 6.88$) 4: ($v > 7.34$)
	4	0: None
	5	0: ($v \leq 5.26$) 1: ($\mu \leq -0.01$) \wedge ($d \leq 0.20$) \wedge ($v > 5.26$) 2: ($\mu \leq -0.01$) \wedge ($d > 0.20$) \wedge ($v > 5.26$) 3: ($\mu > -0.01$) \wedge ($v \leq 6.81$) \wedge ($v > 5.26$) 4: ($\mu > -0.01$) \wedge ($v > 6.81$)
	6	0: ($\delta \leq -0.04$) 1: ($\delta \leq 0.05$) \wedge ($\delta > -0.04$) \wedge ($v \leq 7.81$) 2: ($\delta \leq 0.05$) \wedge ($\delta > -0.04$) \wedge ($v > 7.81$) 3: ($\delta \leq 0.09$) \wedge ($\delta > 0.05$) 4: ($\delta > 0.09$)
	7	0: ($\kappa \leq 0.02$) \wedge ($\mu \leq -0.05$) \wedge ($d \leq 0.61$) 1: ($\kappa \leq 0.02$) \wedge ($\mu > -0.05$) \wedge ($d \leq 0.61$) 2: ($\kappa > 0.02$) \wedge ($d \leq 0.61$) 3: ($\delta \leq 0.06$) \wedge ($\mu \leq -0.04$) \wedge ($d > 0.61$) 4: ($\delta \leq 0.06$) \wedge ($\mu > -0.04$) \wedge ($d > 0.61$) 5: ($\delta > 0.06$) \wedge ($d > 0.61$)

Table S21: Logic program of LSTM in end-to-end visual servoing (Image-based Driving).

Model	Neuron	Logic Program
LSTM	0	0: $(\kappa \leq 0.00) \wedge (d \leq 0.07)$ 1: $(\kappa \leq 0.00) \wedge (d > 0.07)$ 2: $(\kappa \leq 0.00) \wedge (\kappa > 0.00)$ 3: $(\kappa > 0.00) \wedge (v \leq 7.58)$ 4: $(\kappa > 0.00) \wedge (v > 7.58)$
	1	0: $(d \leq -0.08) \wedge (v \leq 7.54)$ 1: $(d \leq 0.04) \wedge (d > -0.08) \wedge (v \leq 7.54)$ 2: $(d \leq 0.04) \wedge (v \leq 7.68) \wedge (v > 7.54)$ 3: $(d \leq 0.04) \wedge (v > 7.68)$ 4: $(d \leq 0.30) \wedge (d > 0.04)$ 5: $(d > 0.30)$
	2	0: $(\kappa \leq 0.00) \wedge (d \leq -0.11)$ 1: $(\kappa > 0.00) \wedge (d \leq -0.11)$ 2: $(d \leq 0.03) \wedge (d > -0.11) \wedge (v \leq 7.50)$ 3: $(d \leq 0.03) \wedge (d > -0.11) \wedge (v > 7.50)$ 4: $(d \leq 0.29) \wedge (d > 0.03)$ 5: $(d > 0.29)$
	3	0: $(v \leq 7.25)$ 1: $(d \leq 0.03) \wedge (v \leq 7.66) \wedge (v > 7.25)$ 2: $(d > 0.03) \wedge (v \leq 7.66) \wedge (v > 7.25)$ 3: $(\delta \leq 0.00) \wedge (v > 7.66)$ 4: $(\delta > 0.00) \wedge (v > 7.66)$
	4	0: $(\delta \leq 0.05) \wedge (\kappa \leq 0.00) \wedge (d \leq 0.23)$ 1: $(\delta \leq 0.05) \wedge (\kappa > 0.00) \wedge (d \leq 0.23)$ 2: $(\delta \leq 0.05) \wedge (d > 0.23)$ 3: $(\delta > 0.05)$
	5	0: $(\delta \leq 0.04)$ 1: $(\delta > 0.04)$
	6	0: None
	7	0: $(\delta \leq -0.01) \wedge (v \leq 7.39)$ 1: $(\delta > -0.01) \wedge (v \leq 7.39)$ 2: $(\kappa \leq 0.02) \wedge (d \leq 0.01) \wedge (v > 7.39)$ 3: $(\kappa > 0.02) \wedge (d \leq 0.01) \wedge (v > 7.39)$ 4: $(d > 0.01) \wedge (v > 7.39)$

Table S22: Logic program of ODE-RNN in end-to-end visual servoing (Image-based Driving).

Model	Neuron	Logic Program
CfC	0	0: $(\delta \leq -0.03) \wedge (\mu \leq 0.02)$ 1: $(\delta > -0.03) \wedge (\mu \leq -0.00)$ 2: $(\delta > -0.03) \wedge (\mu \leq 0.02) \wedge (\mu > -0.00)$ 3: $(\mu > 0.02) \wedge (v \leq 6.79)$ 4: $(\mu > 0.02) \wedge (v > 6.79)$
	1	0: $(\mu \leq -0.05)$ 1: $(\delta \leq -0.03) \wedge (\mu > -0.05)$ 2: $(\delta > -0.03) \wedge (\kappa \leq 0.00) \wedge (\mu > -0.05)$ 3: $(\delta > -0.03) \wedge (\kappa > 0.00) \wedge (\mu > -0.05)$
	2	0: $(\mu \leq 0.02) \wedge (d \leq 0.12) \wedge (v \leq 7.23)$ 1: $(\mu \leq 0.02) \wedge (d \leq 0.12) \wedge (v > 7.23)$ 2: $(\mu \leq 0.00) \wedge (d > 0.12)$ 3: $(\mu \leq 0.02) \wedge (\mu > 0.00) \wedge (d > 0.12)$ 4: $(\mu > 0.02) \wedge (v \leq 6.79)$ 5: $(\mu > 0.02) \wedge (v > 6.79)$
	3	0: $(\delta \leq -0.04)$ 1: (conflict) 2: $(\delta > -0.04) \wedge (d \leq 0.16)$ 3: $(\delta > -0.04) \wedge (d > 0.16)$
	4	0: $(\kappa \leq 0.00) \wedge (\mu \leq -0.00)$ 1: $(\kappa > 0.00) \wedge (\mu \leq -0.00)$ 2: $(\mu \leq 0.02) \wedge (\mu > -0.00) \wedge (d \leq 0.40)$ 3: $(\mu \leq 0.02) \wedge (\mu > -0.00) \wedge (d > 0.40)$ 4: $(\mu > 0.02) \wedge (v \leq 6.87)$ 5: $(\mu > 0.02) \wedge (v > 6.87)$
	5	0: $(v \leq 6.41)$ 1: $(\mu \leq 0.00) \wedge (v \leq 7.15) \wedge (v > 6.41)$ 2: $(\mu \leq 0.00) \wedge (v > 7.15)$ 3: $(\mu > 0.00) \wedge (d \leq 0.51) \wedge (v > 6.41)$ 4: $(\mu > 0.00) \wedge (d > 0.51) \wedge (v > 6.41)$
	6	0: $(\delta \leq -0.00)$ 1: (conflict) 2: $(\delta \leq 0.04) \wedge (\delta > -0.00) \wedge (v \leq 7.18)$ 3: $(\delta \leq 0.04) \wedge (\delta > -0.00) \wedge (v > 7.18)$ 4: $(\delta \leq 0.07) \wedge (\delta > 0.04)$ 5: $(\delta > 0.07)$
	7	0: $(\delta \leq -0.02) \wedge (v \leq 7.26)$ 1: $(\delta > -0.02) \wedge (v \leq 6.56)$ 2: $(\delta > -0.02) \wedge (v \leq 7.26) \wedge (v > 6.56)$ 3: $(\delta \leq 0.00) \wedge (v \leq 7.55) \wedge (v > 7.26)$ 4: $(\delta > 0.00) \wedge (v \leq 7.55) \wedge (v > 7.26)$ 5: $(v > 7.55)$

Table S23: Logic program of CfC in end-to-end visual servoing (Image-based Driving).

Model	Neuron	Logic Program
ODE-RNN	0	0: $(d \leq -0.04) \wedge (v \leq 5.48)$ 1: $(d \leq -0.04) \wedge (v \leq 7.46) \wedge (v > 5.48)$ 2: $(\mu \leq 0.02) \wedge (d > -0.04) \wedge (v \leq 7.46)$ 3: $(\mu > 0.02) \wedge (d > -0.04) \wedge (v \leq 7.46)$ 4: $(\delta \leq 0.05) \wedge (v \leq 7.84) \wedge (v > 7.46)$ 5: $(\delta \leq 0.05) \wedge (v > 7.84)$ 6: $(\delta > 0.05) \wedge (v > 7.46)$
	1	0: $(d \leq -0.72)$ 1: $(d > -0.72) \wedge (v \leq 5.80)$ 2: $(\delta \leq -0.00) \wedge (d > -0.72) \wedge (v > 5.80)$ 3: $(\delta > -0.00) \wedge (d > -0.72) \wedge (v > 5.80)$
	2	0: $(v \leq 5.00)$ 1: $(\delta \leq 0.09) \wedge (v \leq 6.99) \wedge (v > 5.00)$ 2: $(\delta \leq 0.09) \wedge (v > 6.99)$ 3: $(\delta > 0.09) \wedge (v \leq 6.98) \wedge (v > 5.00)$ 4: $(\delta > 0.09) \wedge (v > 6.98)$
	3	0: $(d \leq -0.04)$ 1: $(d \leq 0.04) \wedge (d > -0.04)$ 2: $(\mu \leq -0.11) \wedge (d > 0.04)$ 3: $(\mu > -0.11) \wedge (d \leq 0.92) \wedge (d > 0.04)$ 4: $(\mu > -0.11) \wedge (d > 0.92)$
	4	0: $(\mu \leq 0.02) \wedge (d \leq 0.60) \wedge (v \leq 7.04)$ 1: $(\mu \leq 0.02) \wedge (d > 0.60) \wedge (v \leq 7.04)$ 2: $(\mu > 0.02) \wedge (d \leq -0.43) \wedge (v \leq 7.04)$ 3: $(\mu > 0.02) \wedge (d > -0.43) \wedge (v \leq 7.04)$ 4: $(v \leq 7.53) \wedge (v > 7.04)$ 5: $(d \leq 0.38) \wedge (v > 7.53)$ 6: $(d > 0.38) \wedge (v > 7.53)$
	5	0: $(v \leq 5.38)$ 1: $(\delta \leq -0.03) \wedge (d \leq 0.10) \wedge (v > 5.38)$ 2: $(\delta > -0.03) \wedge (d \leq 0.10) \wedge (v > 5.38)$ 3: $(\delta \leq -0.02) \wedge (d > 0.10) \wedge (v > 5.38)$ 4: $(\delta > -0.02) \wedge (d > 0.10) \wedge (v > 5.38)$
	6	0: $(\mu \leq 0.01) \wedge (d \leq 0.18)$ 1: $(\mu \leq 0.01) \wedge (d \leq 0.47) \wedge (d > 0.18)$ 2: $(\delta \leq 0.10) \wedge (\mu > 0.01) \wedge (d \leq 0.47)$ 3: $(\delta > 0.10) \wedge (\mu > 0.01) \wedge (d \leq 0.47)$ 4: $(d > 0.47) \wedge (v \leq 6.60)$ 5: $(\mu \leq -0.00) \wedge (d > 0.47) \wedge (v > 6.60)$ 6: $(\mu > -0.00) \wedge (d > 0.47) \wedge (v > 6.60)$
	7	0: $(v \leq 5.15)$ 1: $(\mu \leq 0.12) \wedge (d \leq -0.08) \wedge (v > 5.15)$ 2: $(\mu \leq 0.12) \wedge (d > -0.08) \wedge (v > 5.15)$ 3: $(\mu > 0.12) \wedge (v > 5.15)$

Table S24: Logic program of NCP in end-to-end visual servoing (Image-based Driving).

Model	Neuron	Logic Program
NCP	0	0: $(\delta \leq -0.05)$ 1: $(\delta \leq 0.02) \wedge (\delta > -0.05) \wedge (\mu \leq -0.01)$ 2: $(\delta \leq 0.02) \wedge (\delta > -0.05) \wedge (\mu > -0.01)$ 3: $(\delta \leq 0.09) \wedge (\delta > 0.02) \wedge (\mu \leq -0.01)$ 4: $(\delta \leq 0.09) \wedge (\delta > 0.02) \wedge (\mu > -0.01)$ 5: $(\delta > 0.09)$
	1	0: $(\mu \leq 0.05)$ 1: $(\mu > 0.05)$
	2	0: $(\delta \leq 0.02) \wedge (\mu \leq -0.03)$ 1: $(\delta > 0.02) \wedge (\mu \leq -0.03)$ 2: $(\delta \leq -0.02) \wedge (\mu > -0.03)$ 3: $(\delta > -0.02) \wedge (\mu > -0.03)$
	3	0: $(v \leq 7.41)$ 1: $(v \leq 7.72) \wedge (v > 7.41)$ 2: $(d \leq -0.02) \wedge (v > 7.72)$ 3: $(d \leq 0.10) \wedge (d > -0.02) \wedge (v > 7.72)$ 4: $(d > 0.10) \wedge (v \leq 8.05) \wedge (v > 7.72)$ 5: $(d > 0.10) \wedge (v > 8.05)$
	4	0: $(v \leq 7.45)$ 1: $(v \leq 7.78) \wedge (v > 7.45)$ 2: $(v \leq 8.08) \wedge (v > 7.78)$ 3: $(v > 8.08)$
	5	0: $(d \leq -0.15) \wedge (v \leq 7.65)$ 1: $(d \leq -0.15) \wedge (v > 7.65)$ 2: $(\mu \leq 0.06) \wedge (d \leq 0.04) \wedge (d > -0.15)$ 3: $(\mu \leq 0.06) \wedge (d > 0.04)$ 4: $(\mu > 0.06) \wedge (d > -0.15)$
	6	0: $(\delta \leq -0.03) \wedge (v \leq 7.73)$ 1: $(\delta \leq -0.03) \wedge (v > 7.73)$ 2: $(\delta > -0.03) \wedge (\mu \leq 0.07) \wedge (d \leq 0.02)$ 3: $(\delta > -0.03) \wedge (\mu \leq 0.07) \wedge (d > 0.02)$ 4: $(\delta > -0.03) \wedge (\mu > 0.07)$
	7	0: None